Measurement of Beam Profile

The beam width can be changed by focusing via quadruples.
Transverse matching between ascending accelerators is done by focusing.
→ Profiles have to be controlled at many locations.

Synchrotrons: Lattice functions ***β(s)*** and ***D(s)*** are fixed ⇒ width ***σ*** and emittance ***ε*** are:

$$\sigma_x^2(s) = \varepsilon_x \beta_x(s) + \left(D(s) \frac{\Delta p}{p} \right)^2 \quad \text{and} \quad \sigma_y^2(s) = \varepsilon_y \beta_y(s) \quad \text{(no vertical bend)}$$

LINACs: Lattice functions are ‘smoothly’ defined due to variable input emittance.

Typical beam sizes:

e^--beam: typically Ø 0.1 to 3 mm, **protons:** typically Ø 1 to 30 mm

A great variety of devices are used:

- ***Optical techniques**:* Scintillating screens (all beams),
  synchrotron light monitors (e–), optical transition radiation (e–),
  residual gas fluorescence monitors (protons), ionization profile monitors (protons).
- ***Electronics techniques:*** Secondary electron emission (SEM) grids, wire scanners (all)

Outline:

- **Scintillation screens:**
  emission of light, universal usage, limited dynamic range
- **SEM-Grid**
- **Wire scanner**
- **Ionization Profile Monitor and Beam Induced Fluorescence Monitor**
- **Optical Transition Radiation**
- **Synchrotron Light Monitors**
- **Summary**

Scintillation screens are used from the 'early days' on e.g. by Ernest Rutherford in 1911:

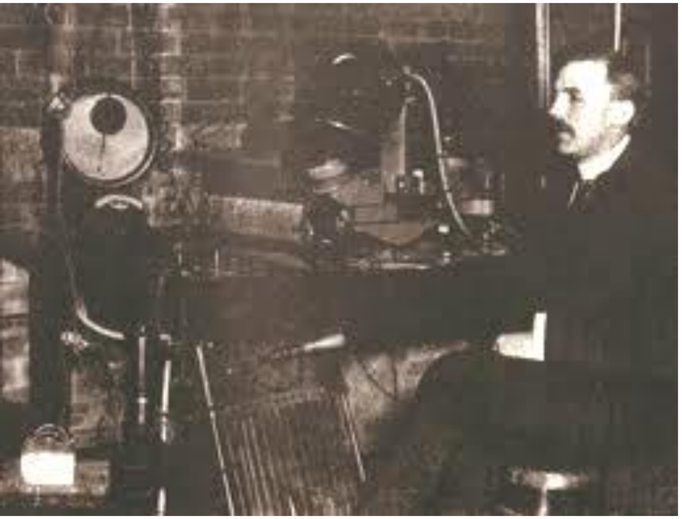

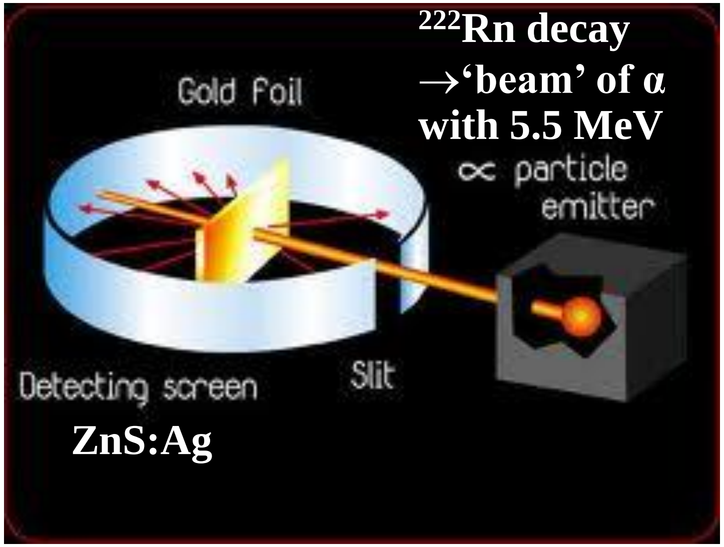

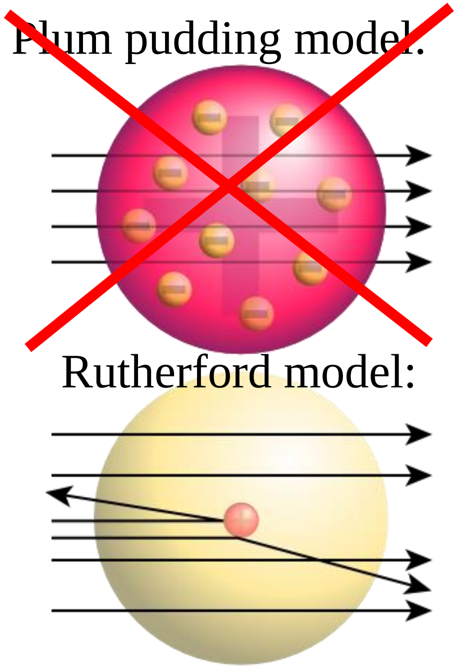

Rutherford or 'Geiger-Marsden Experiment':

- Nuclei are made of point-like charges

ZnS:Ag

- light emitter excited by the energy release by charged particle → sintillation
- today known as Phosphor P11 and is used in TV tubes etc.

Particle's energy loss in matter produces light

→ the most direct way of profile observation as used from the early days on!

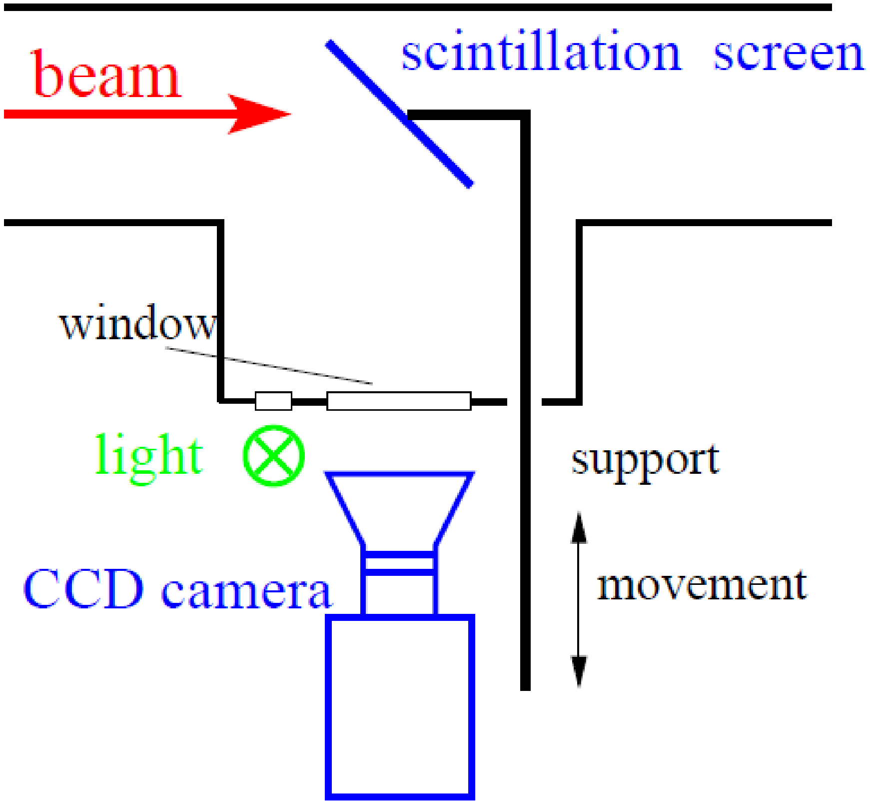

Pneumatic feed-through with Ø70 mm screen :

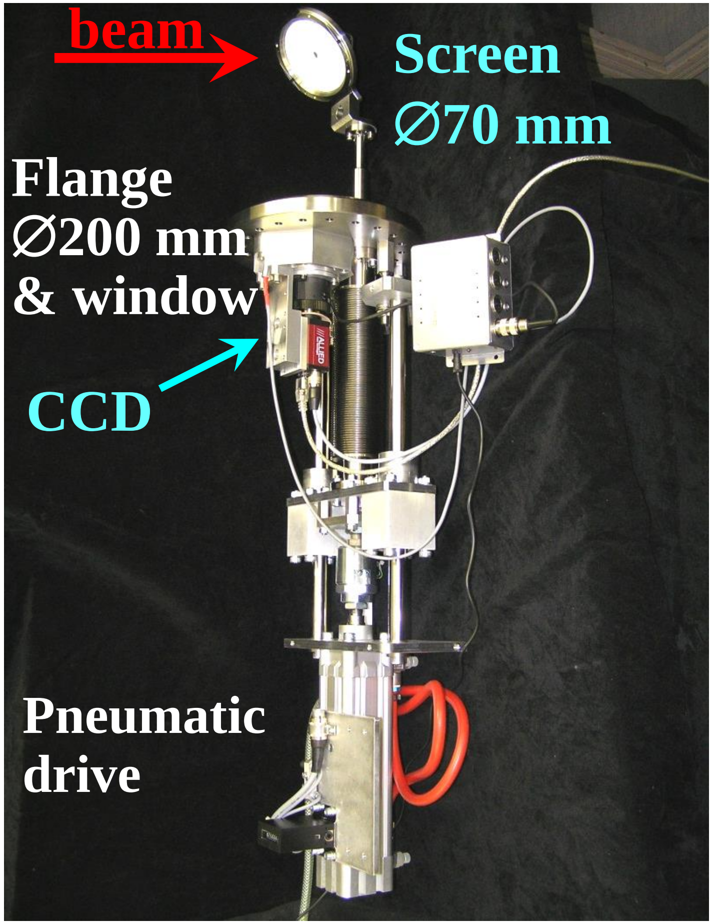

Example of Screen based Beam Profile Measurement

Example: GSI LINAC, 4 MeV/u, low current, YAG:Ce screen

Advantage of screens:

- ➢Direct 2-dim measurement
- ➢High spatial resolution
- ➢Cheap realization

Observation with

a CCD or CMOS camera

 with digital output

or video & frame grabber.

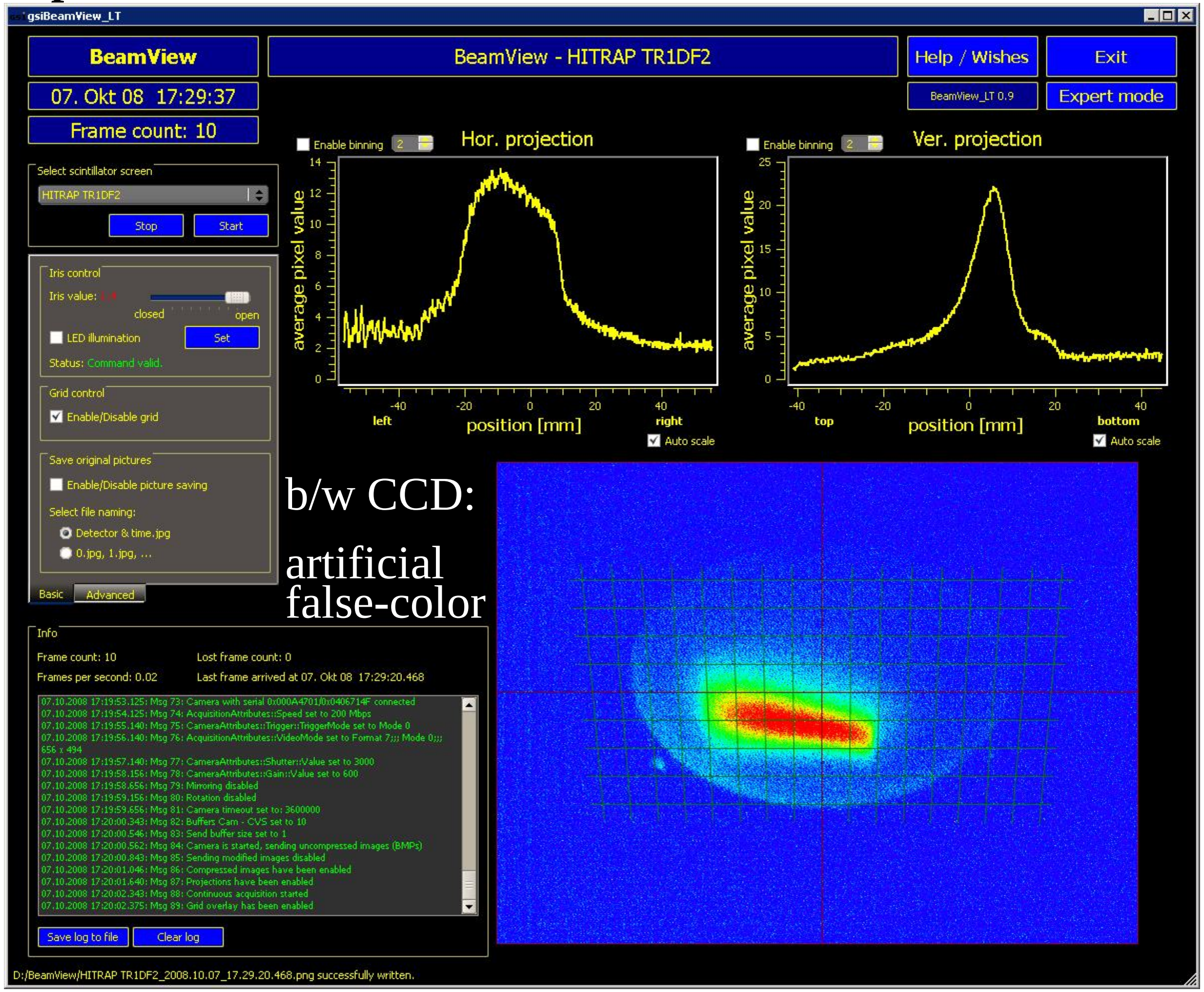

b/w CCD:

artificial false-color

Light output from various Scintillating Screens

Example: Color CCD camera: Images at different particle intensities determined for U at 300 MeV/u

Al_2O_3

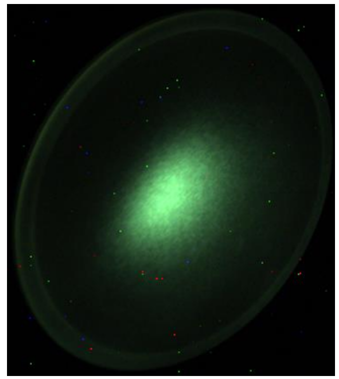

CsI:Tl

Al_2O_3:Cr

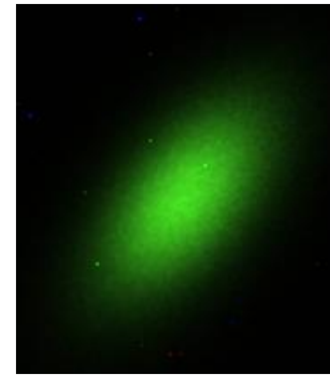

P43

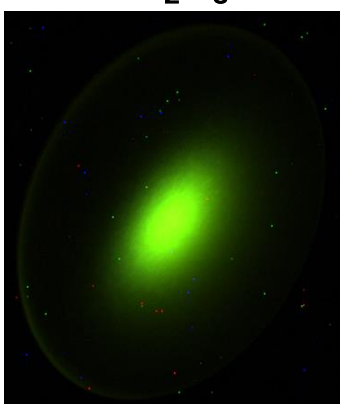

YAG:Ce

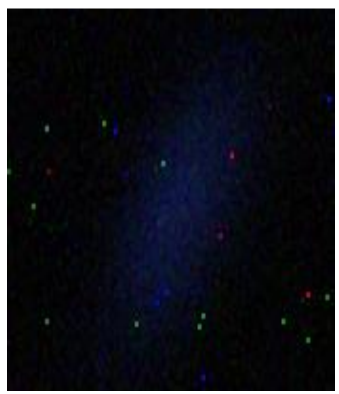

Herasil

Quartz:Ce

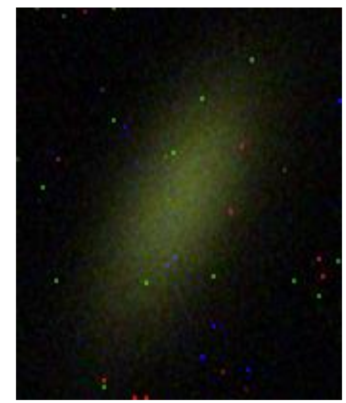

ZrO_2:Mg

- Very different light yield i.e. photons per ion‘s energy loss
- Different wavelength of emitted light

Interaction steps within the scintillation process

- beam interaction

→ hot electrons + deep holes

- multiplication:

electron – electron scattering

- thermalization:

electron – phonon coupling

- capture at doped atom and/or electron - hole pair creation

- emission of photons

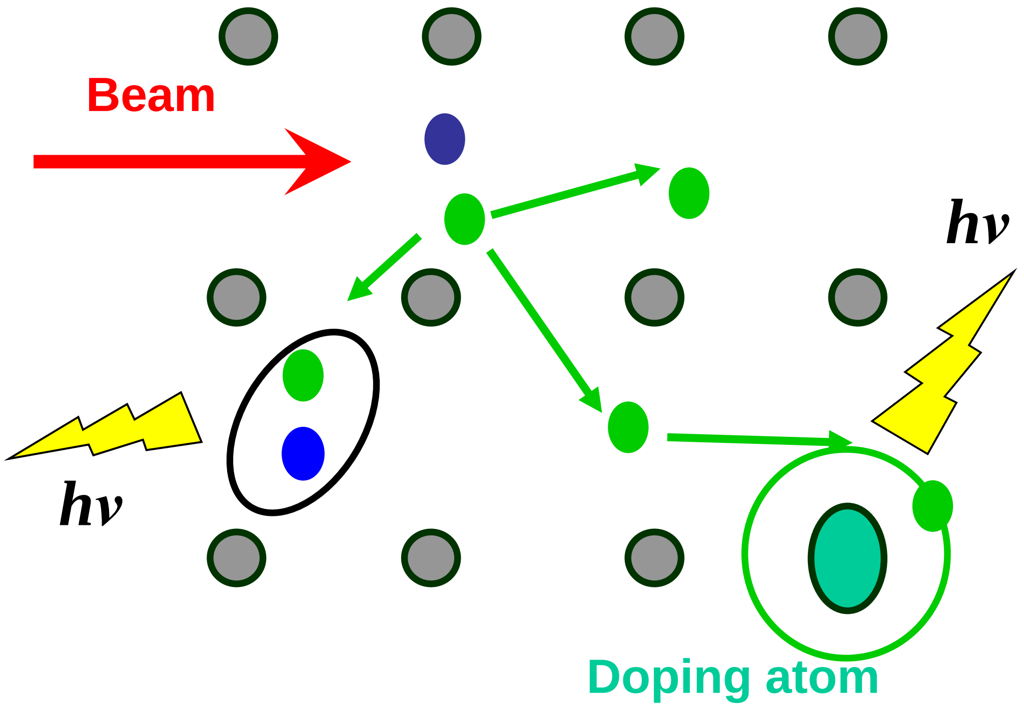

Wavelength Spectrum for Scintillation Screens

Wavelength spectrum of Al_2O_3:Cr (Chromox)

→ Emission is dominated by Chromium dopant

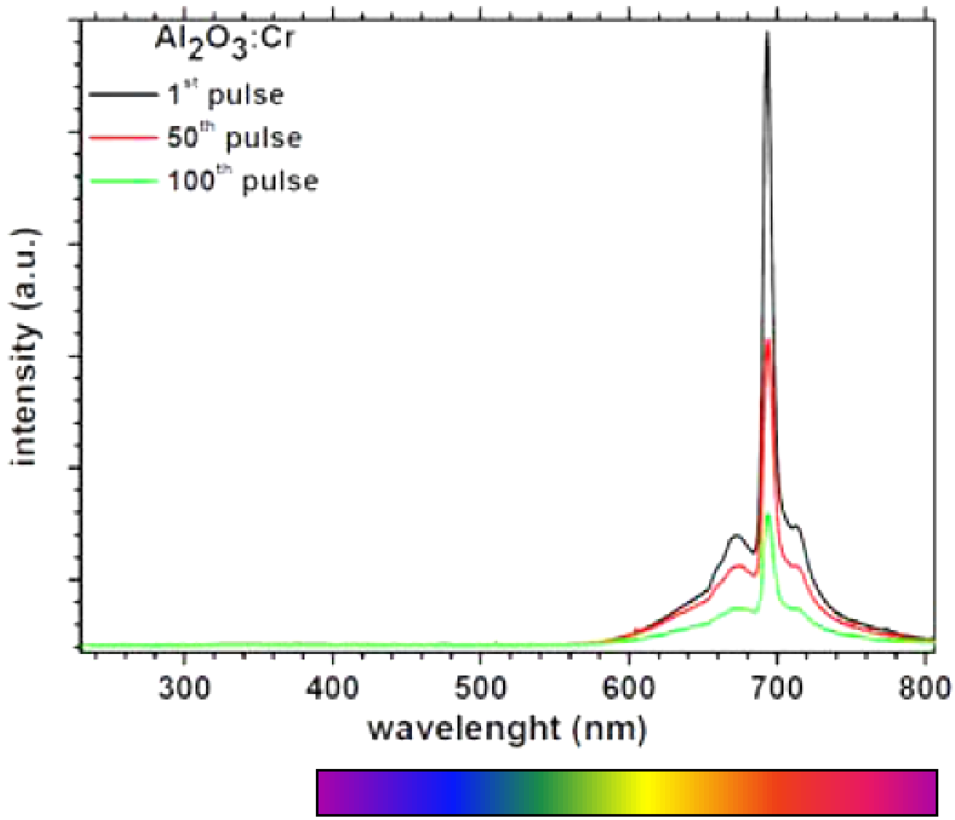

Other materials have different spectra

→ Optimization to sensitivity of detector

→ but others material properties

have to obeyed and weighted

Beam parameters: $^{238}U^{28+}$, 4.8 MeV/u, **5 · 10^{10} ppp** in 500 µs, ~450 µA

[E. Gütlich (GSI) et al., BIW 2010]

Some materials and their basic properties:

Name	**Type**	**Material**	**Activ.**	**Max. λ**	**Decay**
Chromox	Cera-mics	Al_2O_3	Cr	700 nm	≈ 10 ms
Alumina		Al_2O_3	Non	380 nm	≈ 10 ns
YAG:Ce	Crystal	$Y_3Al_5O_{12}$	Ce	550 nm	200 ns
P43	Powder	Gd_2O_3S	Tb	545 nm	1 ms
P46		$Y_3Al_5O_{12}$	Ce	530 nm	300 ns
P47		$Y_3Si_5O_{12}$	Ce&Tb	400 nm	100 ns

Standard drive with P43 screen

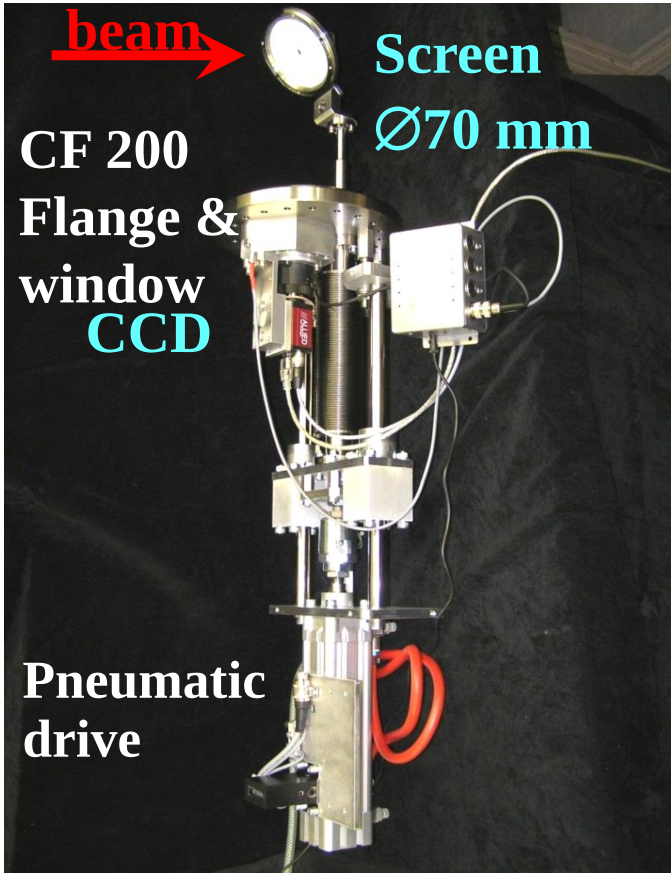

Properties of a good scintillator:

- Large light output at optical wavelength
  → standard CCD camera can be used
- Large dynamic range → usable for different ions
- Short decay time → observation of variations
- Radiation hardness → long lifetime
- Good mechanical properties → typ. size up to Ø 10 cm

(Phosphor Pxx grains of Ø ≈ 10 μm on glass or metal).

Example: Light Output from various Screens

Example: Beam images for various scintillators irradiated by Uranium at ≈ 300 MeV/u at GSI

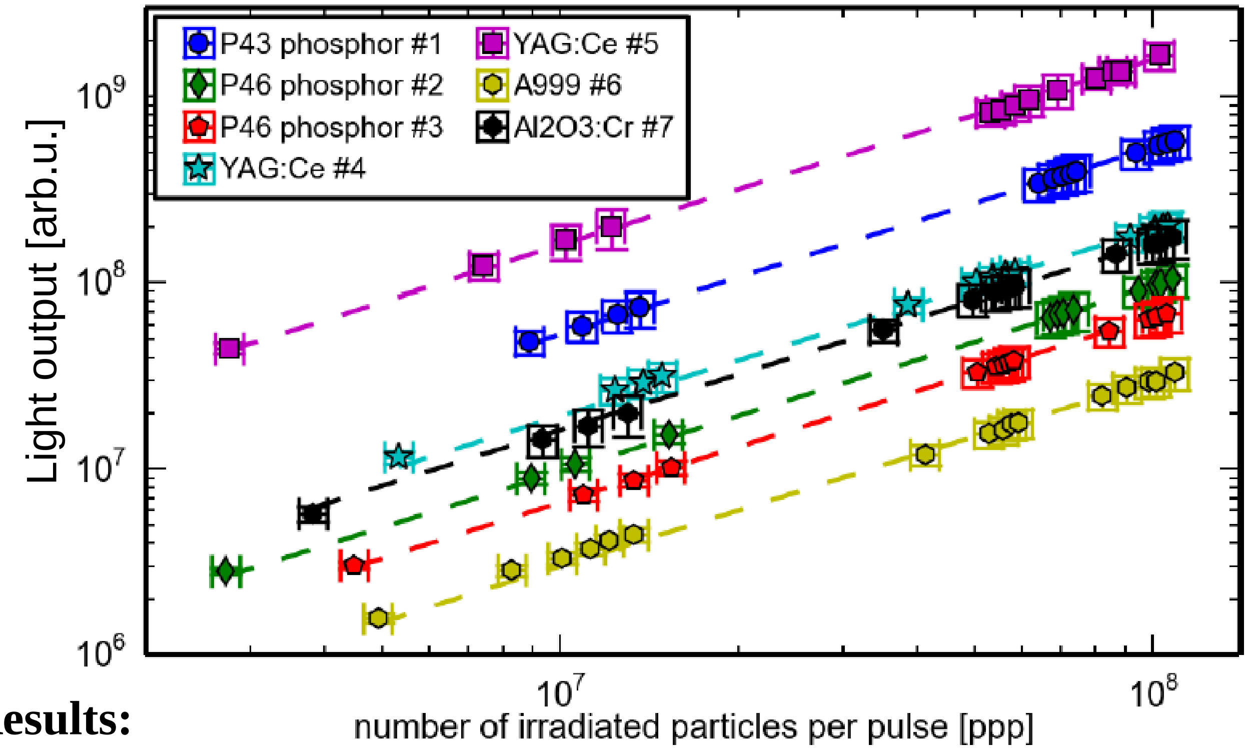

From P. Forck et al., IPAC'14,

A. Lieberwirth et al., NIM B 2015

Results:

- Several orders of magnitude different light output
- ⇒ material matched to beam intensity must be chosen
- Well suited: powder phosphor screens P43 and P46
- → cheap, can be sedimeted on large substrates of nearly any shape
- Light output linear with respect to particles per pulse

Outline:

- Scintillation screens:
  emission of light, universal usage, limited dynamic range
- SEM-Grid: emission of electrons, workhorse, limited resolution
- Wire scanner
- Ionization Profile Monitor and Beam Induced Fluorescence Monitor
- Optical Transition Radiation
- Synchrotron Light Monitors
- Summary

Excurse: Secondary Electron Emission by Ion Impact

Energy loss of ions in metals close to a surface:

Closed collision with large energy transfer: → fast e^- with E_{kin} >> 100 eV

Distant collision with low energy transfer → slow e^- with $E_{kin} \lesssim$ 10 eV

→ 'diffusion' & scattering with other e^-: scattering length $L_s \approx$ 1 - 10 nm

→ at surface ≈ 90 % probability for escape

Secondary **electron yield** and energy distribution comparable for all metals!

$$\Rightarrow \quad Y = const. * dE/dx$$ (Sternglass formula)

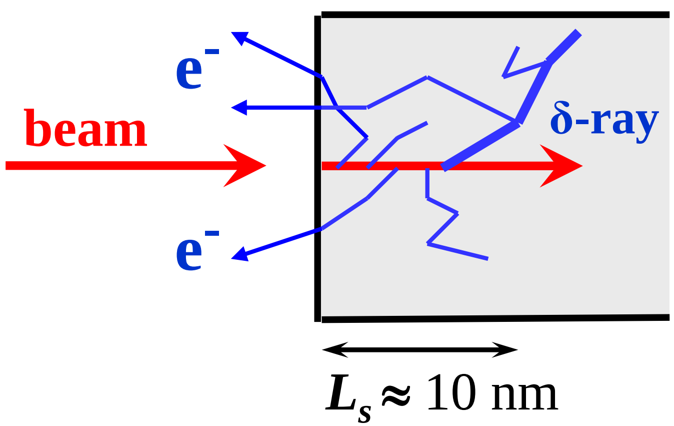

Different targets:

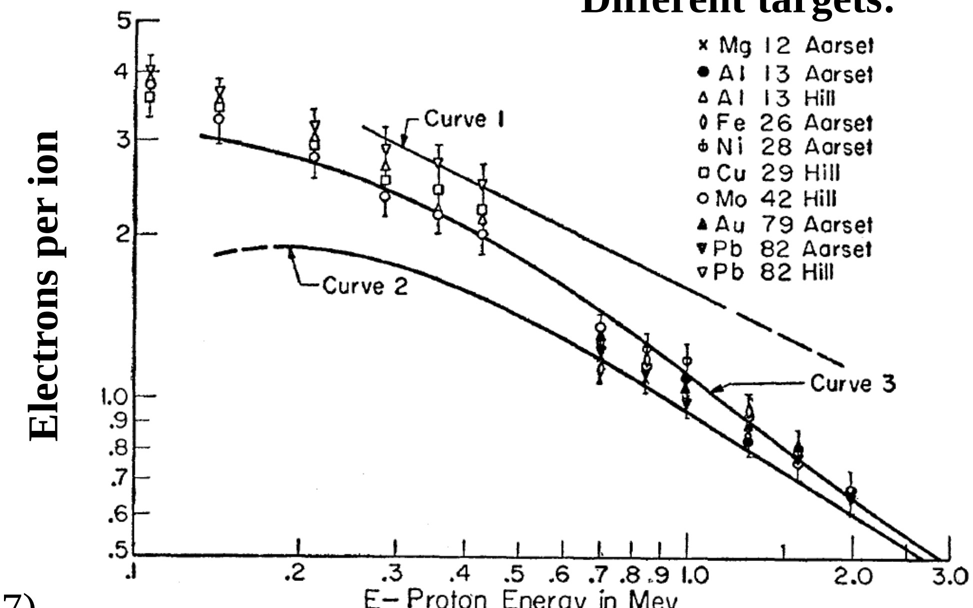

From E.J. Sternglass, Phys. Rev. 108, 1 (1957)

Secondary Electron Emission Grids = SEM-Grid

Beam surface interaction: e⁻ emission → measurement of current.

Example: 15 wire spaced by 1.5 mm:

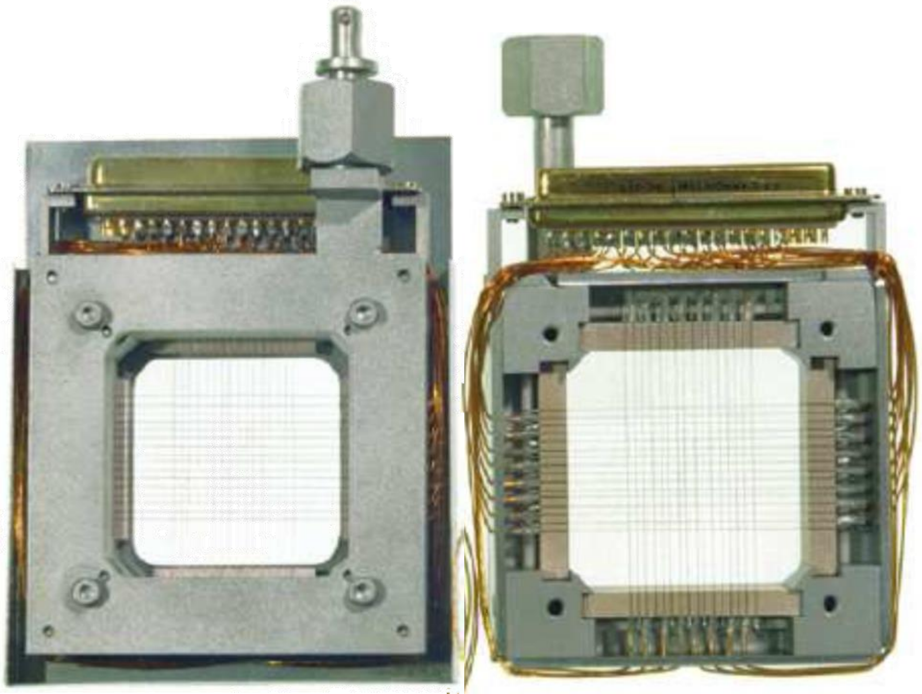

SEM-Grid feed-through on CF200:

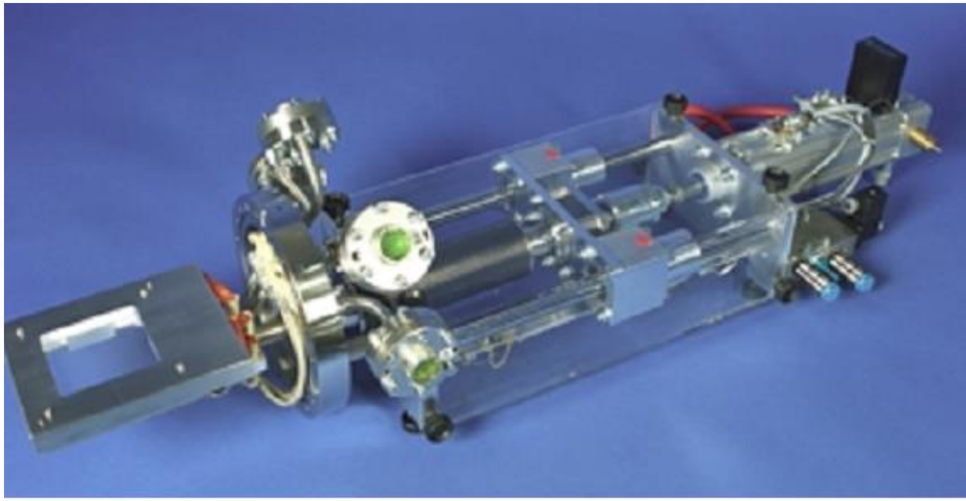

Beam surface interaction: e⁻ emission → measurement of current.

Example: 15 wire spaced by 1.5 mm:

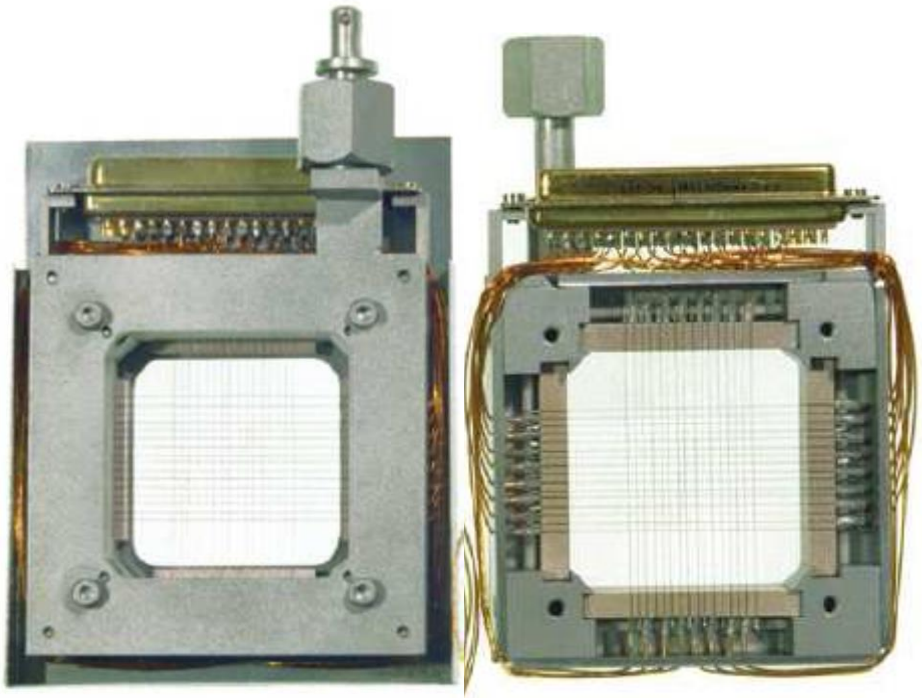

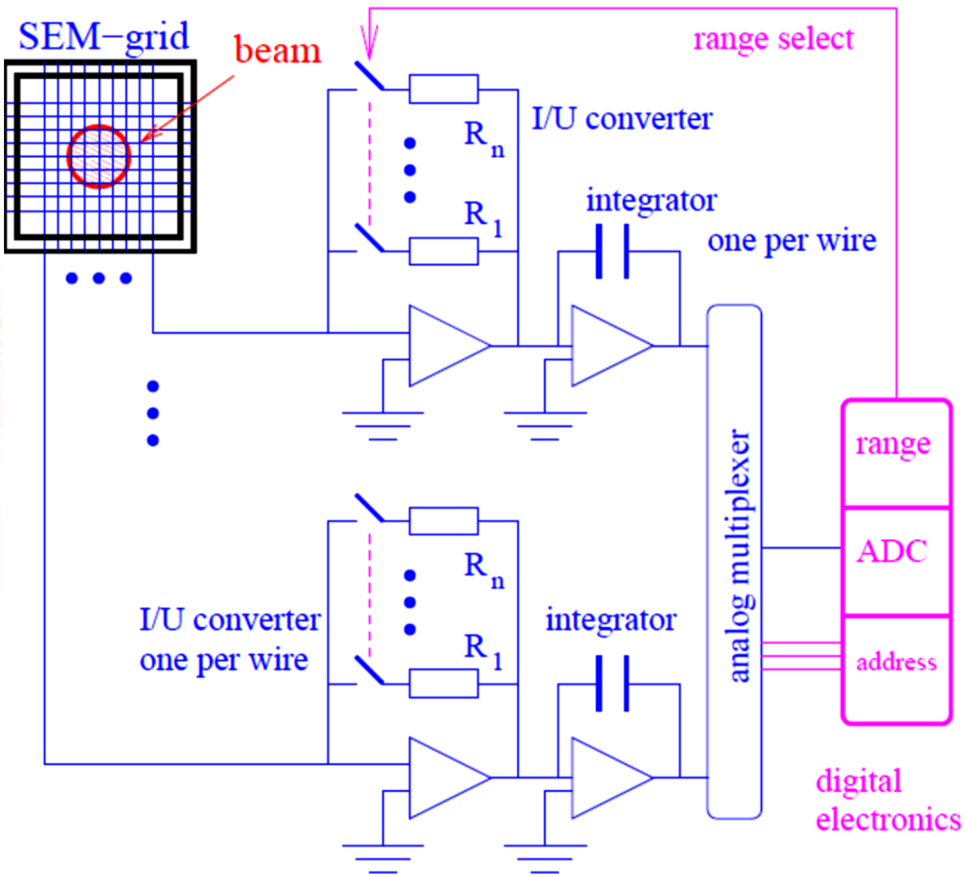

Each wire is equipped with one I/U converter different ranges settings by R_i
→ very large dynamic range up to 10^6.

The Artist view of a SEM-Grid = Harp

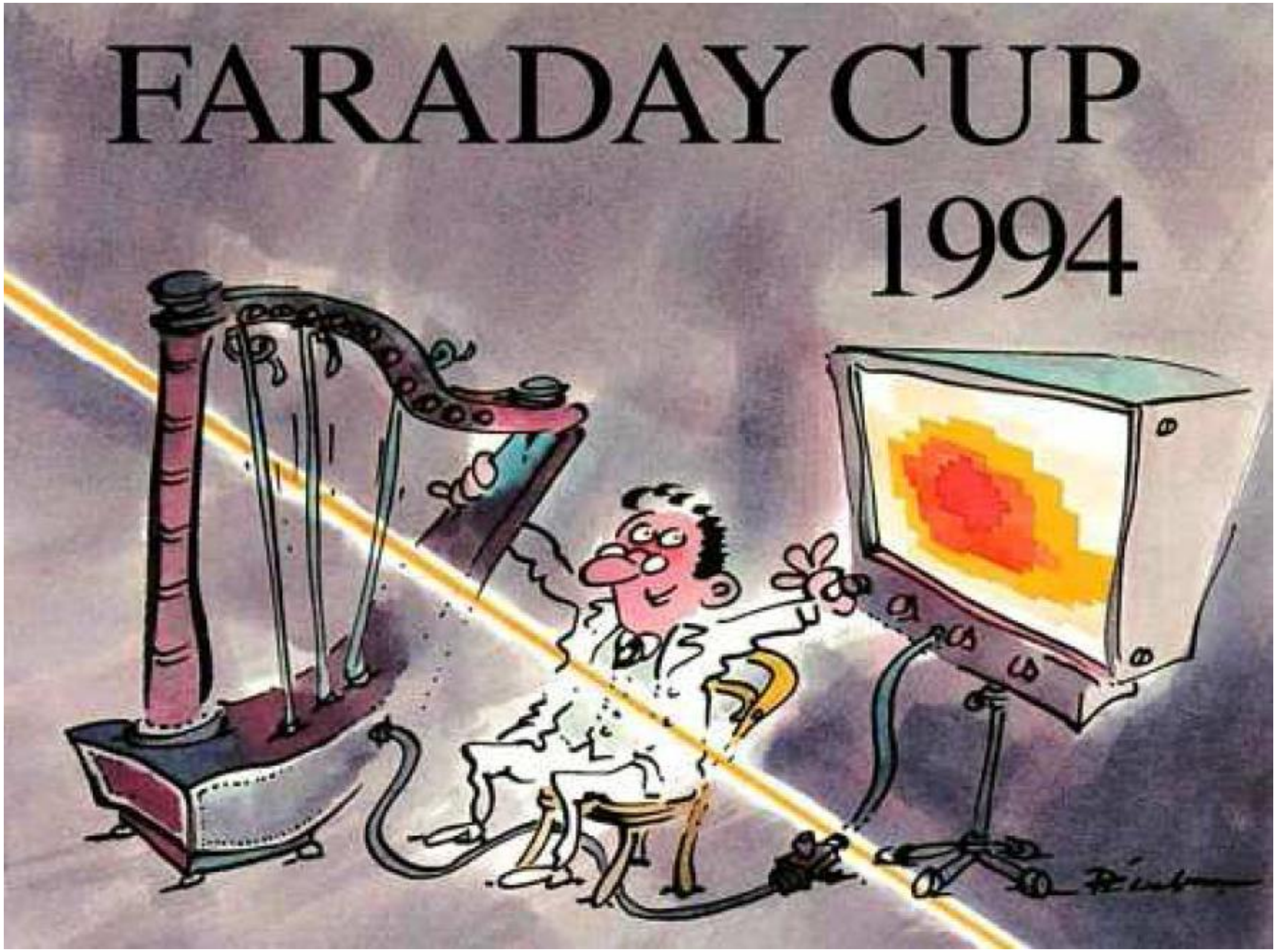

The Faraday Cup is an award granded every second year for beam diagnostics inventions .

Properties of a SEM-Grid

Secondary e- emission from wire or ribbons, 10 to 100 per plane.

Specifications for SEM-Grids at the GSI-LINAC:

Diameter of the wires	0.05 to 0.5 mm
Spacing	0.5 to 2 mm
Length	50 to 100 mm
Material	W or W-Re alloy
Insulation of the frame	glass or Al_2O_3
number of wires	10 to 100
Max. power rating in vacuum	1 W/mm
Min. sensitivity of I/U-conv.	1 nA/V
Dynamic range	$1:10^6$
Number of ranges	10 typ.
Integration time	1 μs to 1 s

Example: Ribbon type SEM-Grid

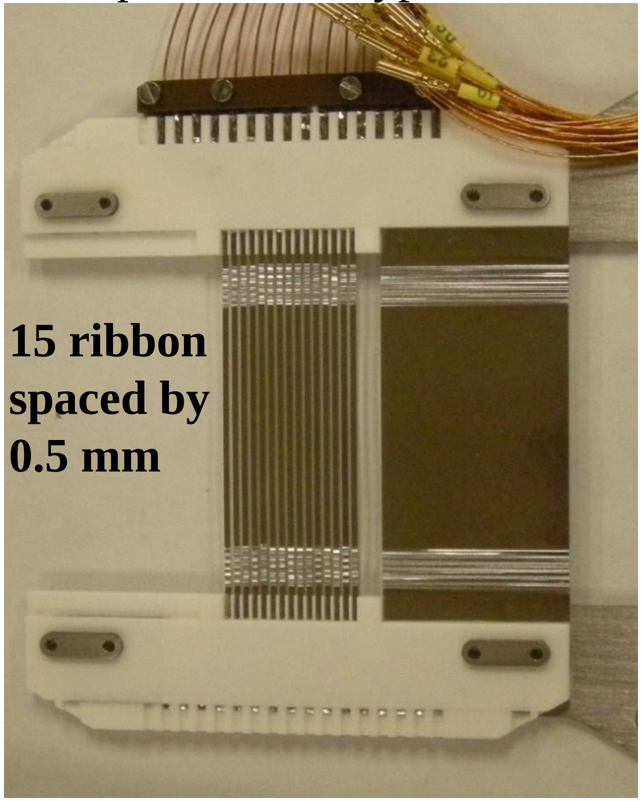

Care has to be taken to prevent over-heating by the energy loss!

Low energy beam: **Wires** with ratio of spacing/width: ≃ 1mm/0.1mm = 10 → only 10 % loss.

High energy E_{kin} > 1 GeV/u: typ. 25 μm thick **ribbons** & 0.5 mm width → negligible energy loss.

Example of Profile Mesurement with SEM-Grids

Even for low energies, several SEM-Grid can be used due to the ≈80 % transmission

⇒ frequently used instrument beam optimization: setting of quadrupoles, energy….

Example: C^{6+} beam of 11.4 MeV/u at different locations at GSI-LINAC

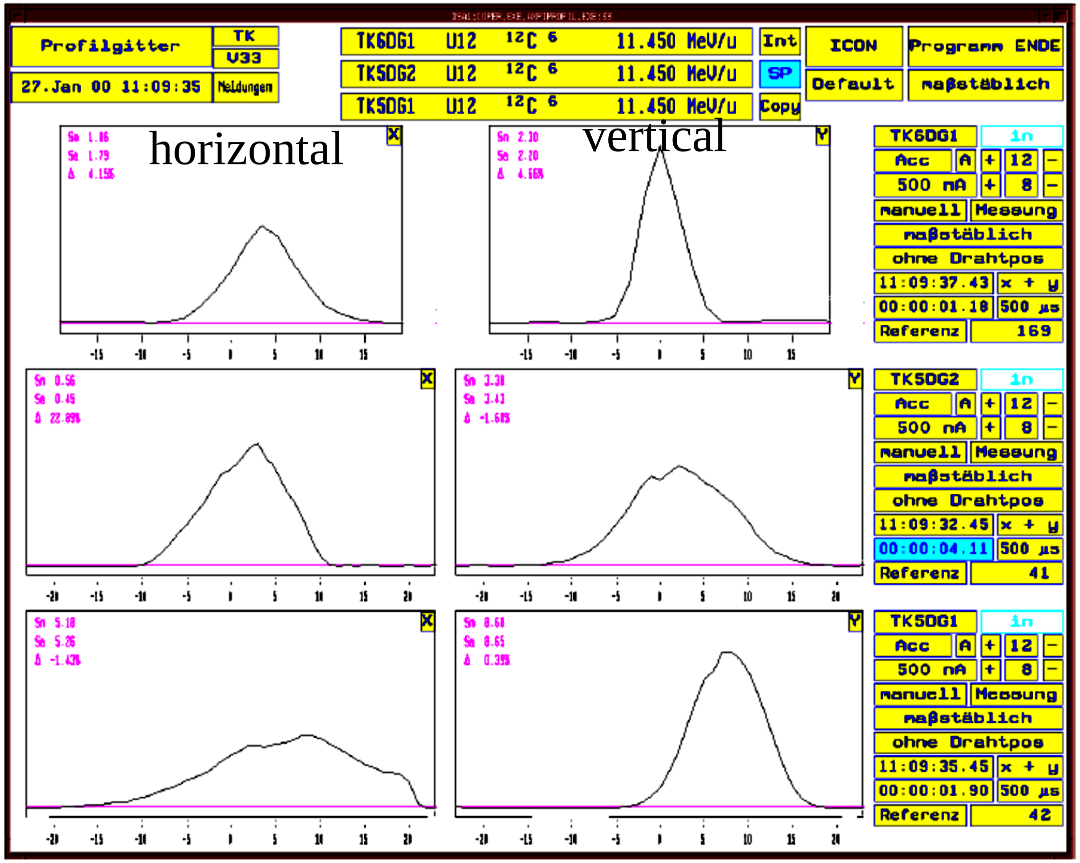

Outline:

- Scintillation screens:
  emission of light, universal usage, limited dynamic range
- SEM-Grid: emission of electrons, workhorse, limited resolution
- **Wire scanner:** emission of electrons, workhorse, scanning method
- Ionization Profile Monitor and Beam Induced Fluorescence Monitor
- Optical Transition Radiation
- Synchrotron Light Monitors
- Summary

Slow, linear Wire Scanner

Idea: One wire is scanned through the beam!

Slow, linear scanner are used for:

- low energy protons
- high resolution measurements e.g. at e^+-e^- colliders
  by de-convolution $\sigma^2_{beam}=\sigma^2_{meas}-d^2_{wire}$
  $\Rightarrow$ resolution down to µm can be reached
- detection of beam halo.

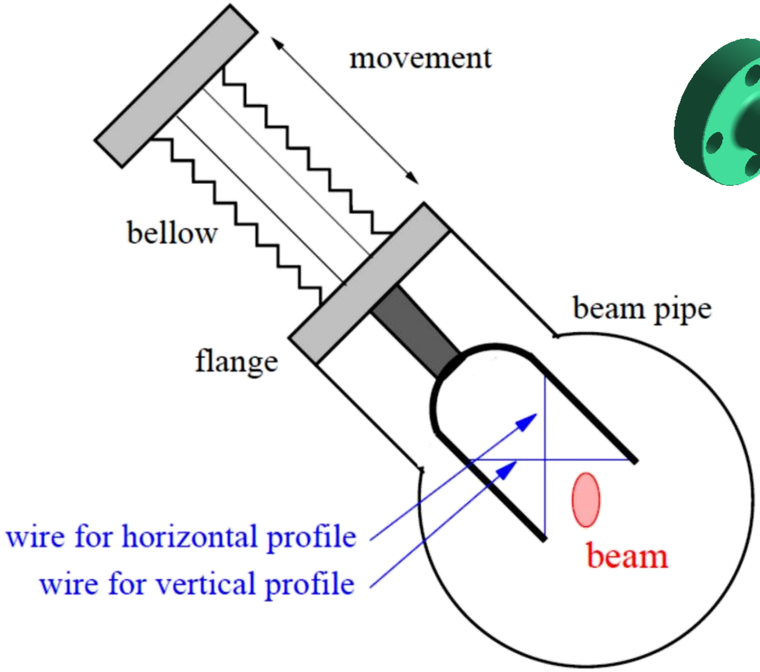

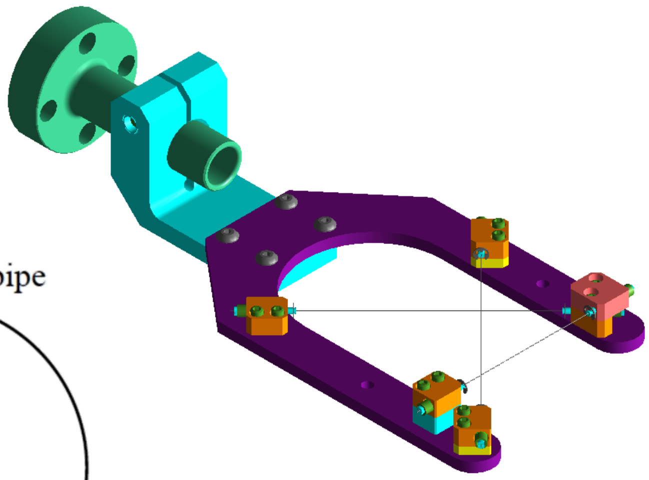

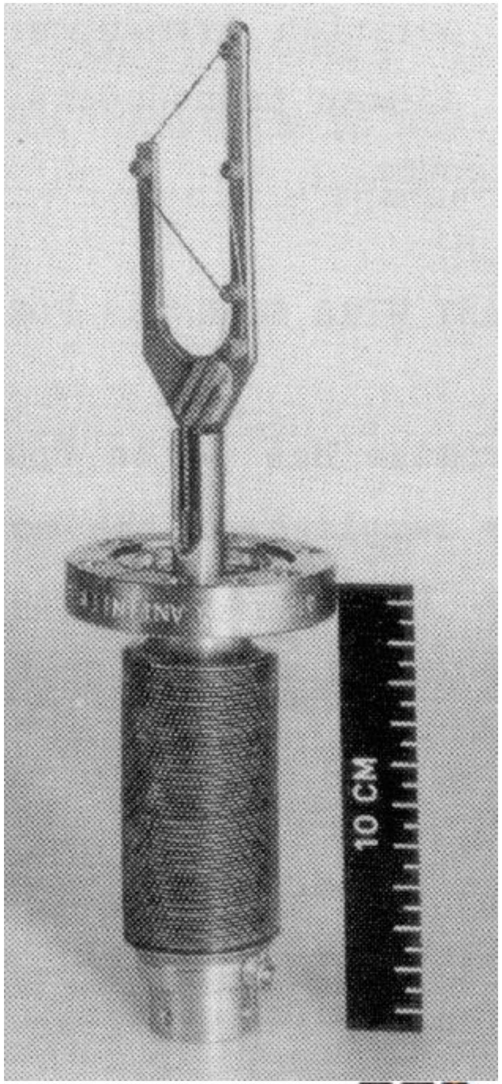

Idea: One wire is scanned through the beam!

Slow, linear scanner are used for:

- low energy protons
- high resolution measurements e.g. at e^+-e^- colliders
  by de-convolution $\sigma^2_{beam}=\sigma^2_{meas}-d^2_{wire}$
  $\Rightarrow$ resolution down to μm can be reached
- detection of beam halo.

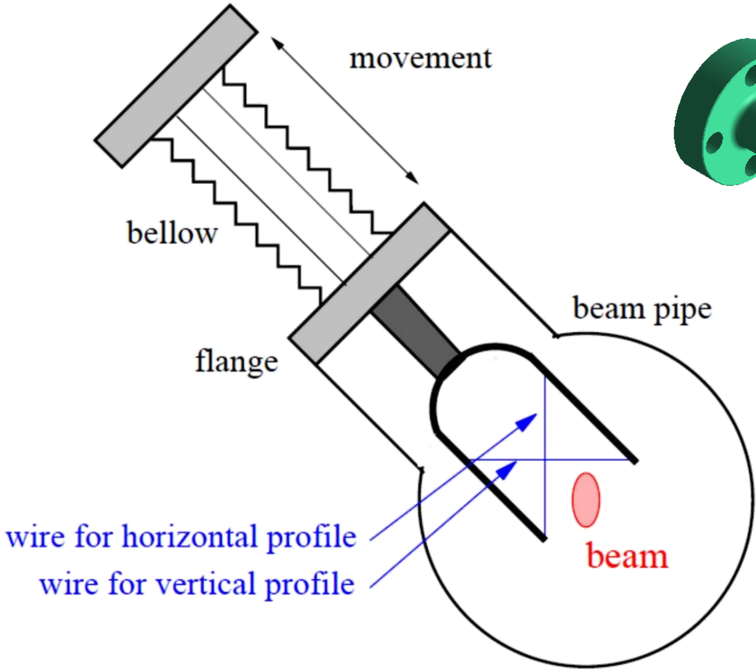

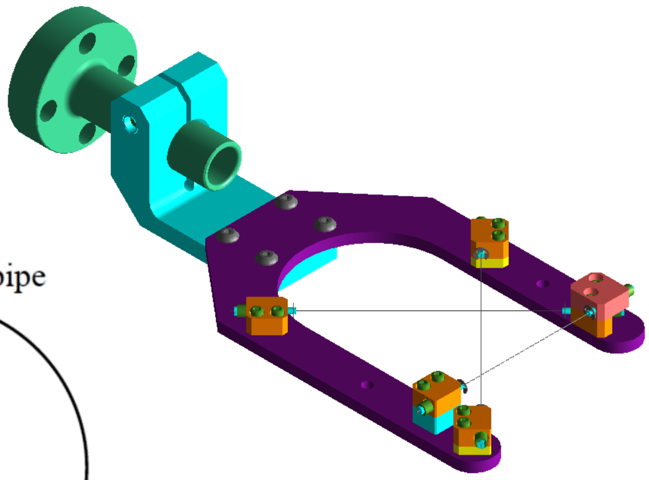

Instead of several wires, ***one*** wire is scanned though the beam.

Fast pendulum scanner for synchrotrons; sometimes it is called ***'flying wire'***:

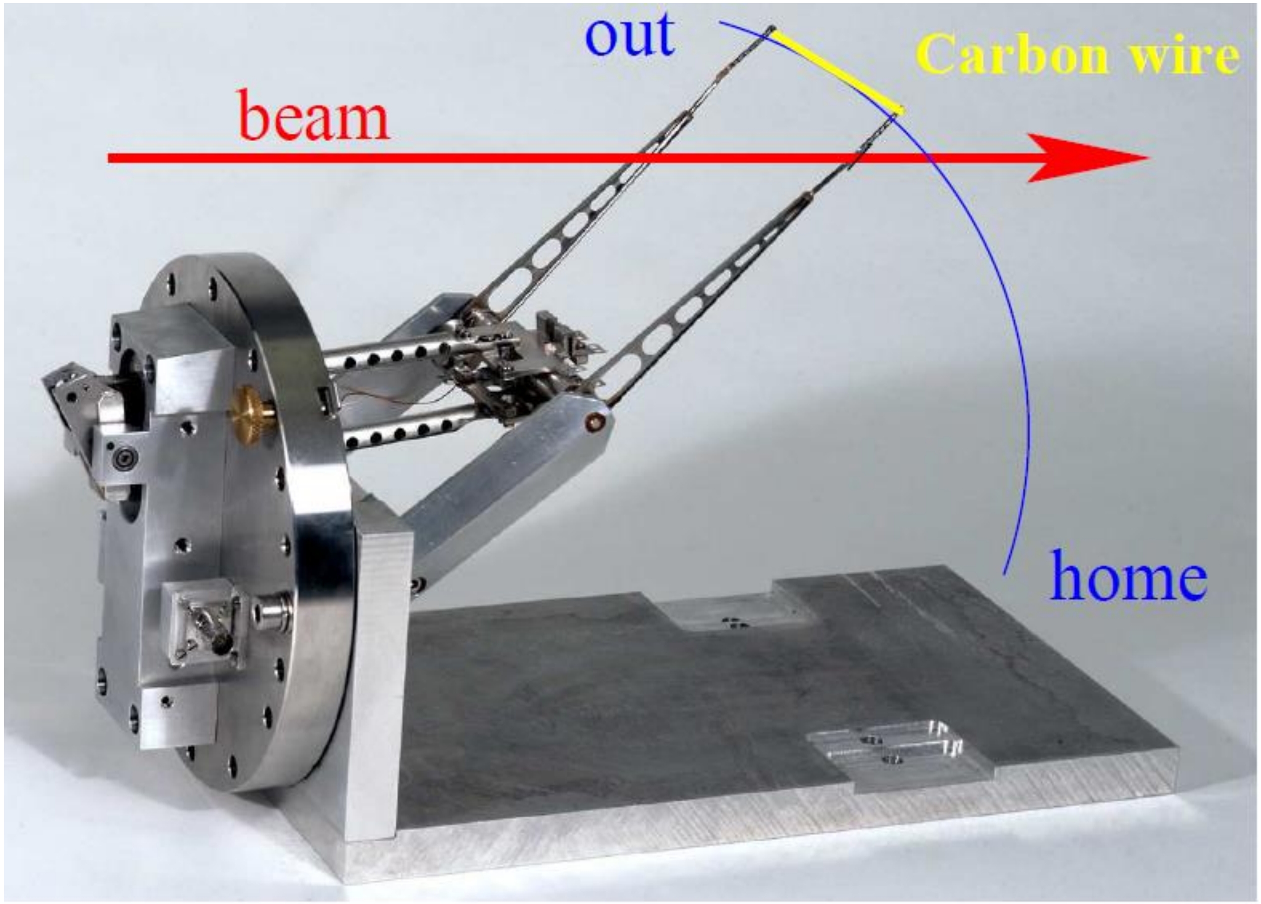

Usage of Wire Scanners

Material: carbon or SiC → low Z-material for low energy loss and high temperature.

Thickness: down to 10 μm → high resolution.

Detection: Either the **secondary current** (like SEM-grid) or
high energy **secondary particles** (like beam loss monitor)
flying wire: only sec. particle detection due to induced current by movement.

Secondary particles:

Proton beam → hadrons shower (π, n, p...)

Electron beam → Bremsstrahlung photons.

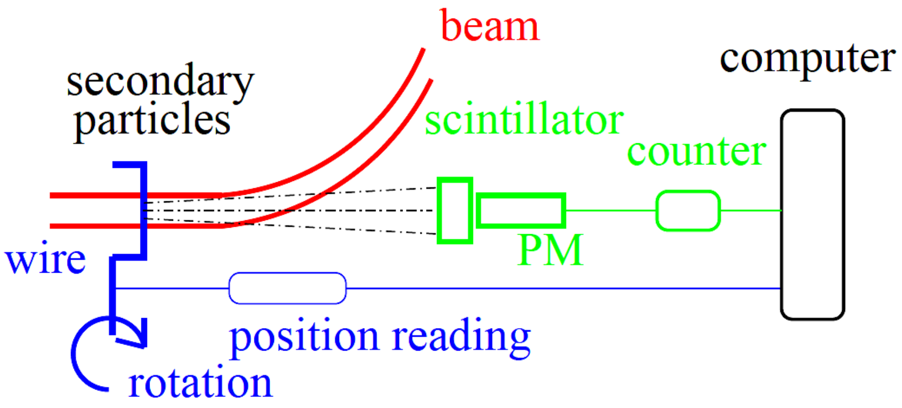

Proton impact on scanner at CERN-PS Booster:

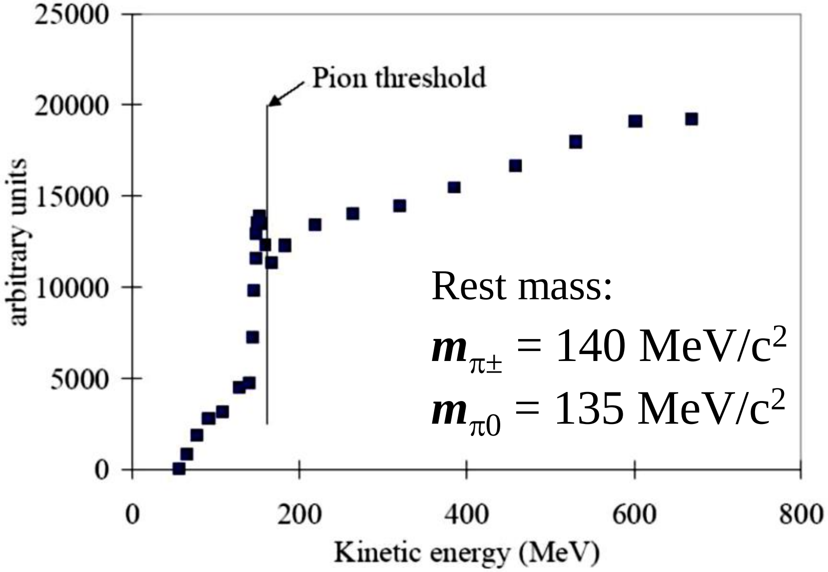

Kinematics of flying wire:

Velocity during passage typically 10 m/s = 36 km/h and typical beam size ∅ 10 mm

⇒ time for traversing the beam $t \approx 1$ **ms**

The Artist View of a Wire Scanner

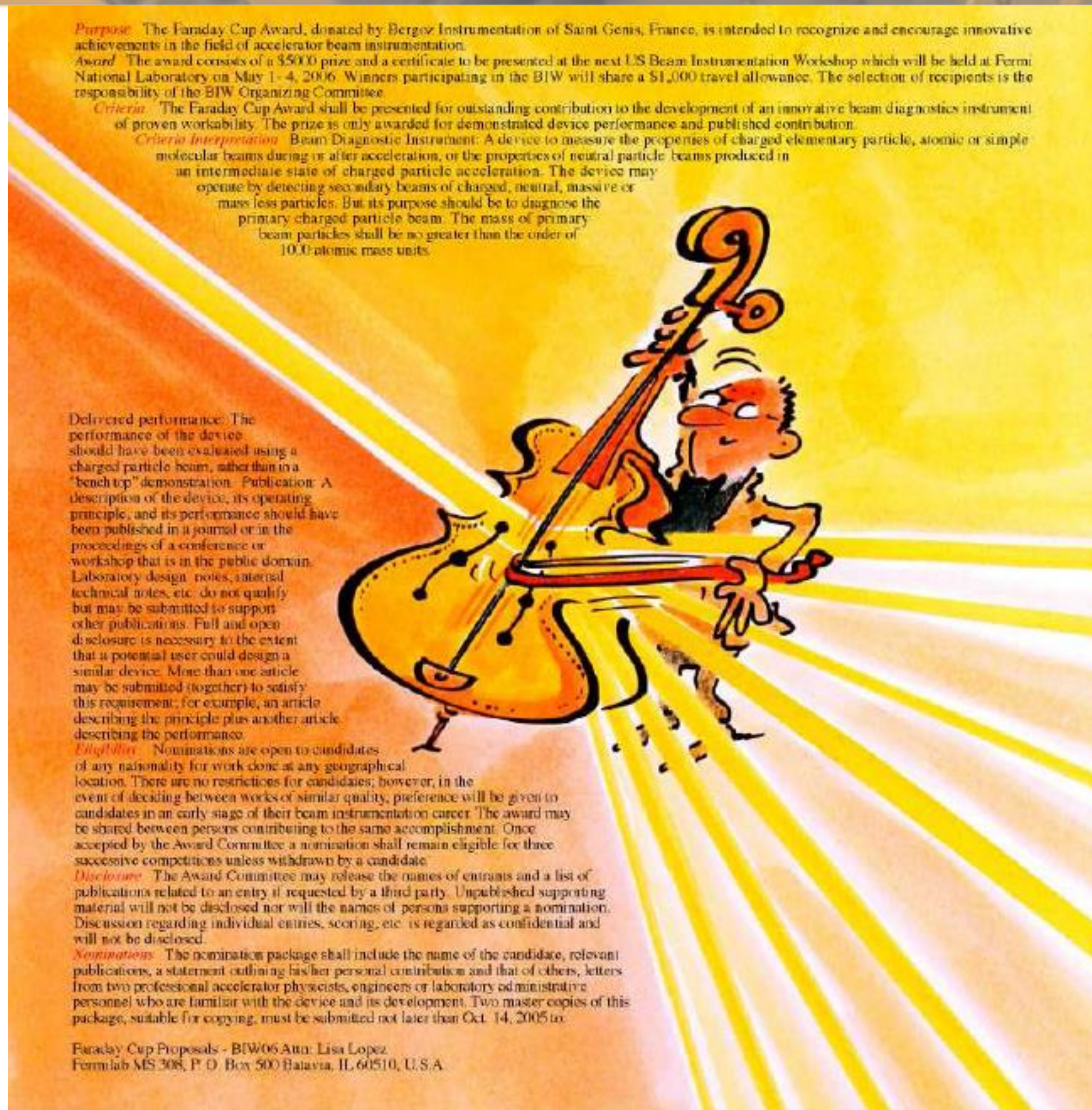

Comparison between SEM-Grid and Wire Scanners

Grid: Measurement at a single moment in time

Scanner: Fast variations can not be monitored

→ for pulsed LINACs precise synchronization is needed

Grid: Not adequate at synchrotrons for stored beam parameters

Scanner: At high energy synchrotrons flying wire scanners are nearly non-destructive

---

Grid: Resolution of a grid is fixed by the wire distance (typically 1 mm)

Scanner: For slow scanners the resolution is about the wire thickness (down to 10 μm)

→ used for e−-beams having small sizes (down to 10 μm)

Grid: Needs one electronics channel per wire

→ expensive electronics and data acquisition

Scanner: Needs a precise movable feed-through → expensive mechanics.

Outline:

- Scintillation screens:
  emission of light, universal usage, limited dynamic range
- SEM-Grid: emission of electrons, workhorse, limited resolution
- Wire scanner: emission of electrons, workhorse, scanning method
- Ionization Profile Monitor and Beam Induced Fluorescence Monitor:
  secondary particle detection from interaction beam-residual gas
- Optical Transition Radiation
- Synchrotron Light Monitors
- Summary

Non-destructive device for proton synchrotron:

- beam ionizes the residual gas by electronic stopping
- gas ions or e^- accelerated by E -field ≈1 kV/cm
- spatial resolved single particle detection

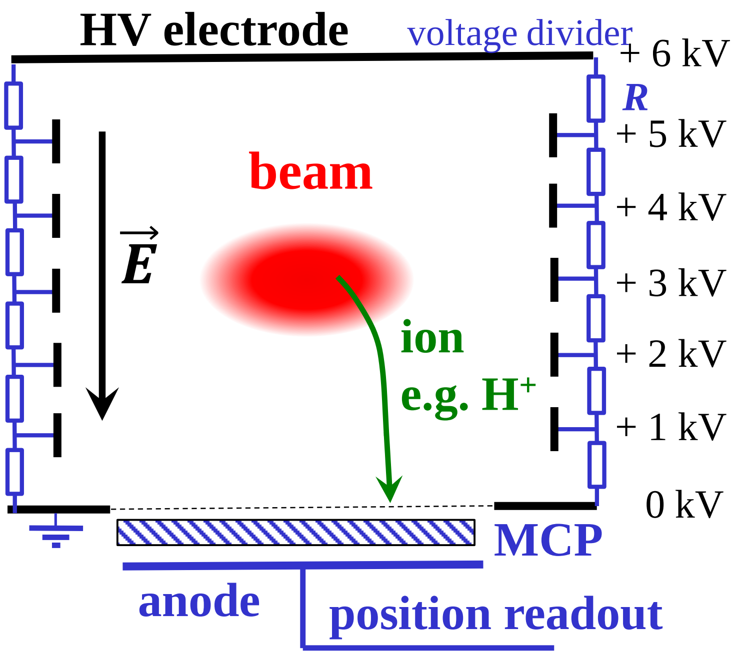

IPM for the use at the GSI LINAC:
Vacuum p ≃ 10^{-7} mbar, I ≃ 1 mA
Readout by strips fed to an I/U converter.

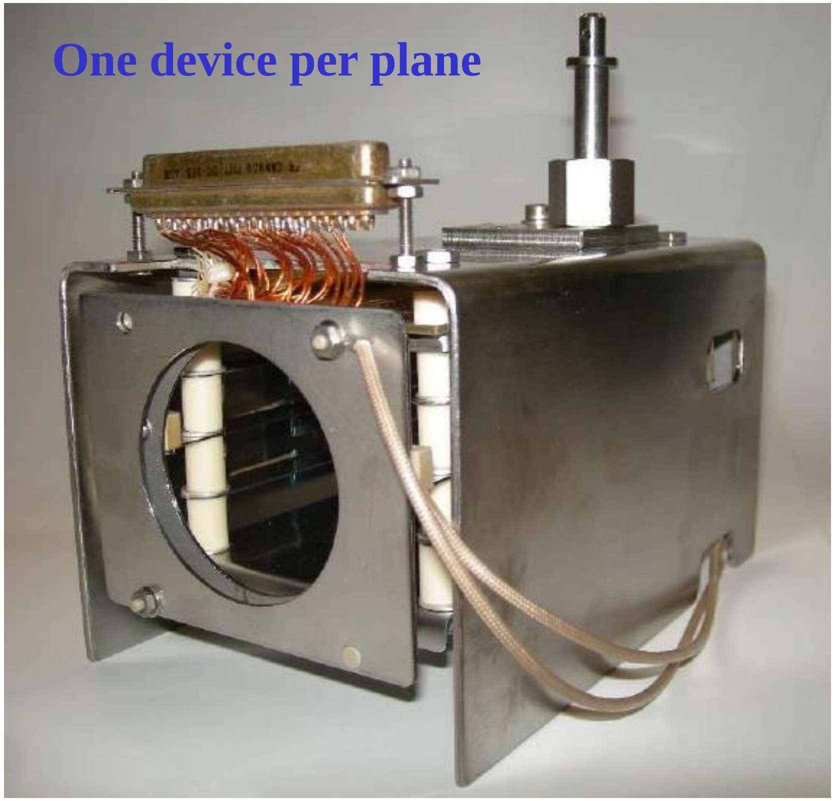

Typical vacuum pressure:
Transfer line: N_2 $10^{-8}...10^{-6}$ mbar ≅ $3\cdot10^{8}...3\cdot10^{10}\text{cm}^{-3}$
Synchrotron: H_2 $10^{-11}...10^{-9}$ mbar ≅ $3\cdot10^{5}...3\cdot10^{7}\text{cm}^{-3}$

Ionization Profile Monitor at GSI Synchrotron

Non-destructive device for proton synchrotron:

- beam ionizes the residual gas by electronic stopping
- gas ions or e⁻ accelerated by E -field ≈1 kV/cm
- spatial resolved single particle detection

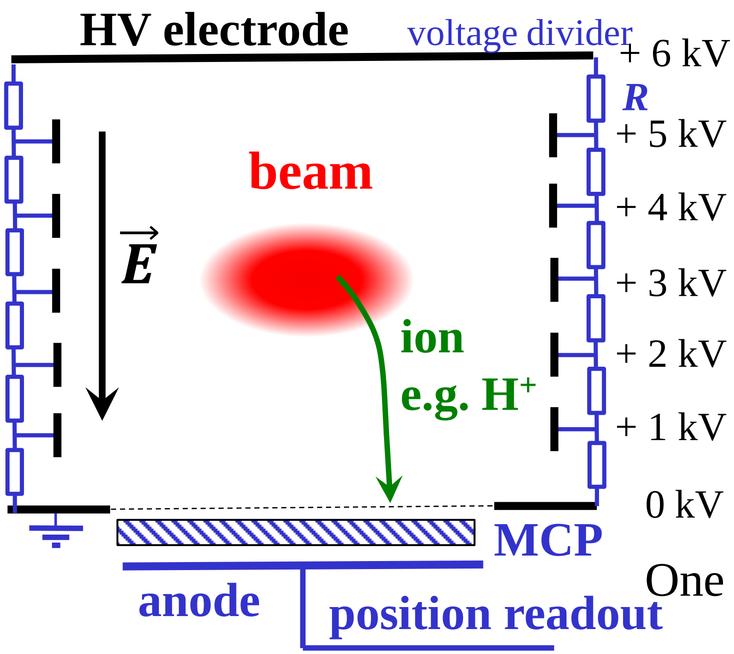

One device per plane

Realization at GSI synchrotron:

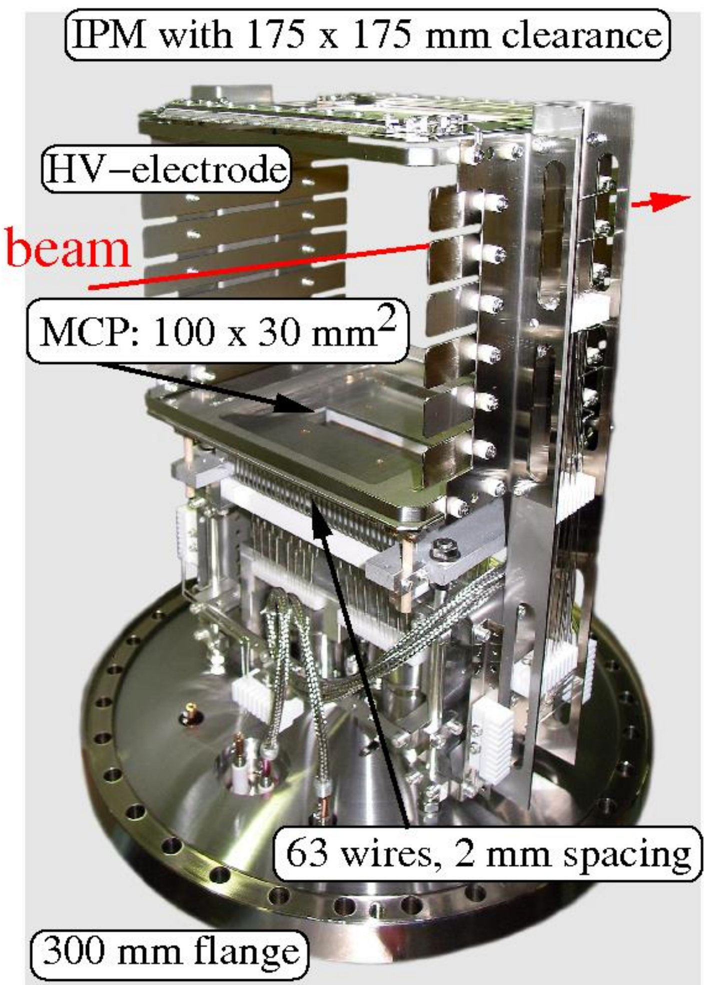

Typical vacuum pressure:

Transfer line: N_2 $10^{-8}...10^{-6}$ mbar $\cong 3\cdot10^{8}...3\cdot10^{10}$ cm^{-3}

Synchrotron: H_2 $10^{-11}...10^{-9}$ mbar $\cong 3\cdot10^{5}...3\cdot10^{7}$ cm^{-3}

The realization for the heavy ion storage ring ESR at GSI:

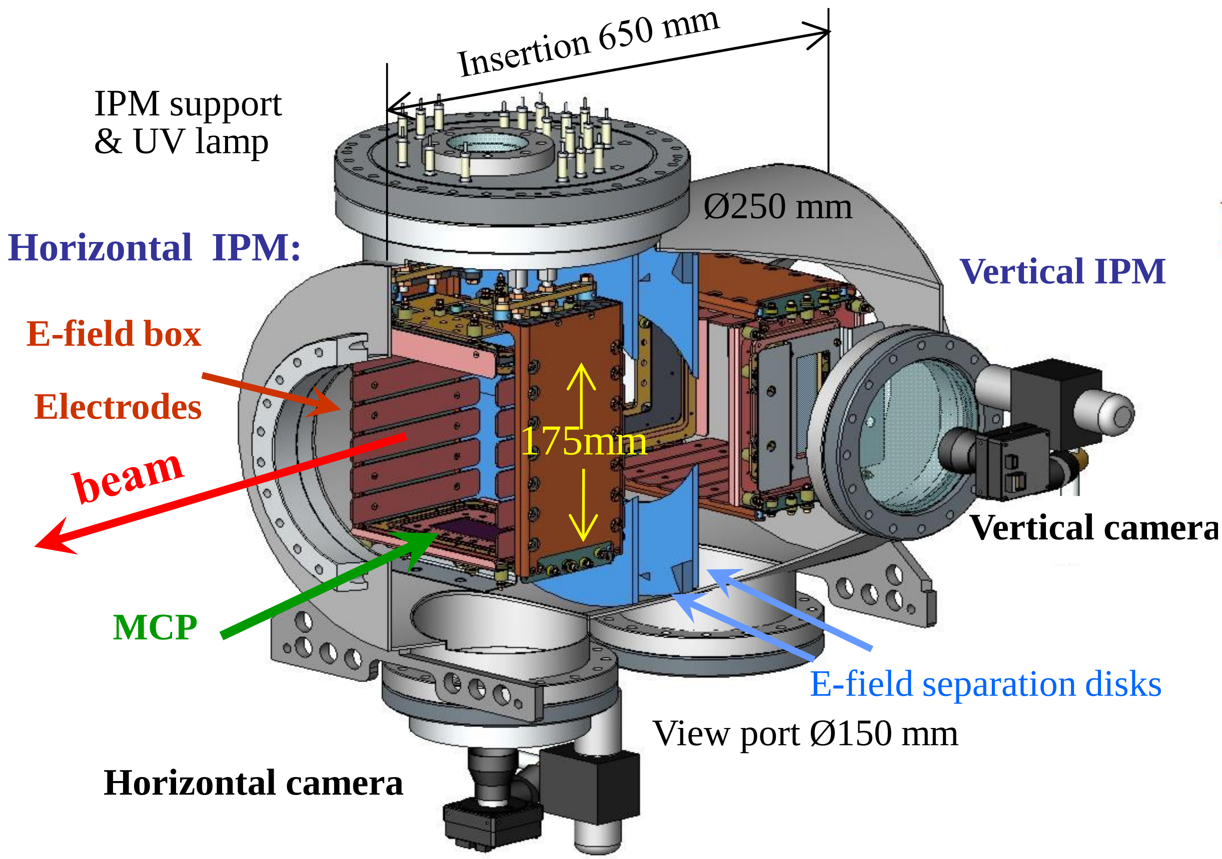

Realization at GSI synchrotron:

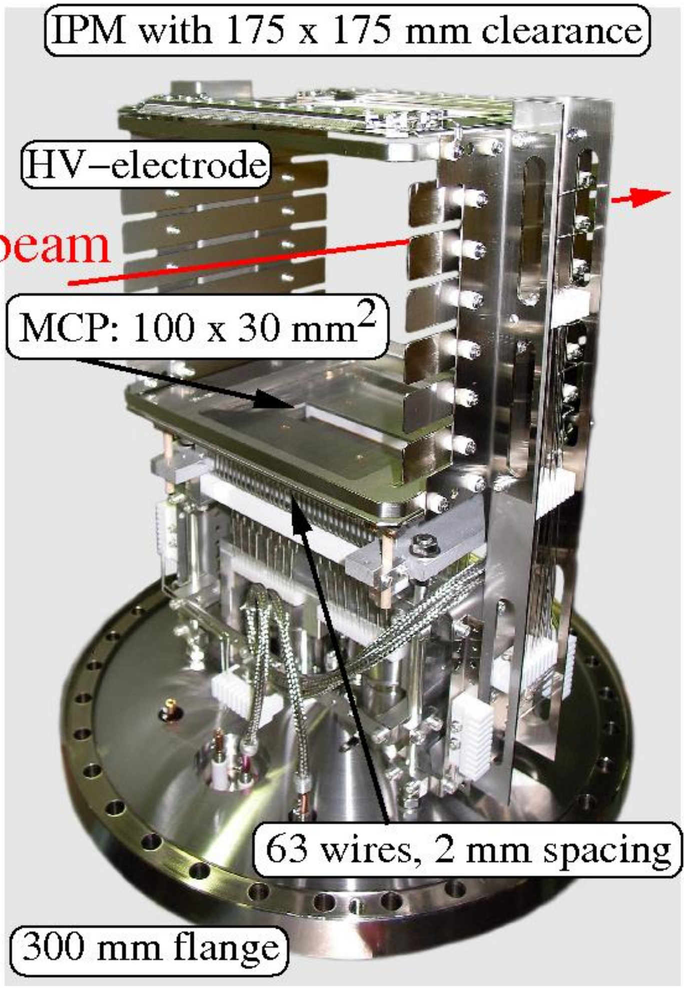

Ionization Profile Monitor Realization

The realization for the heavy ion storage ring ESR at GSI:

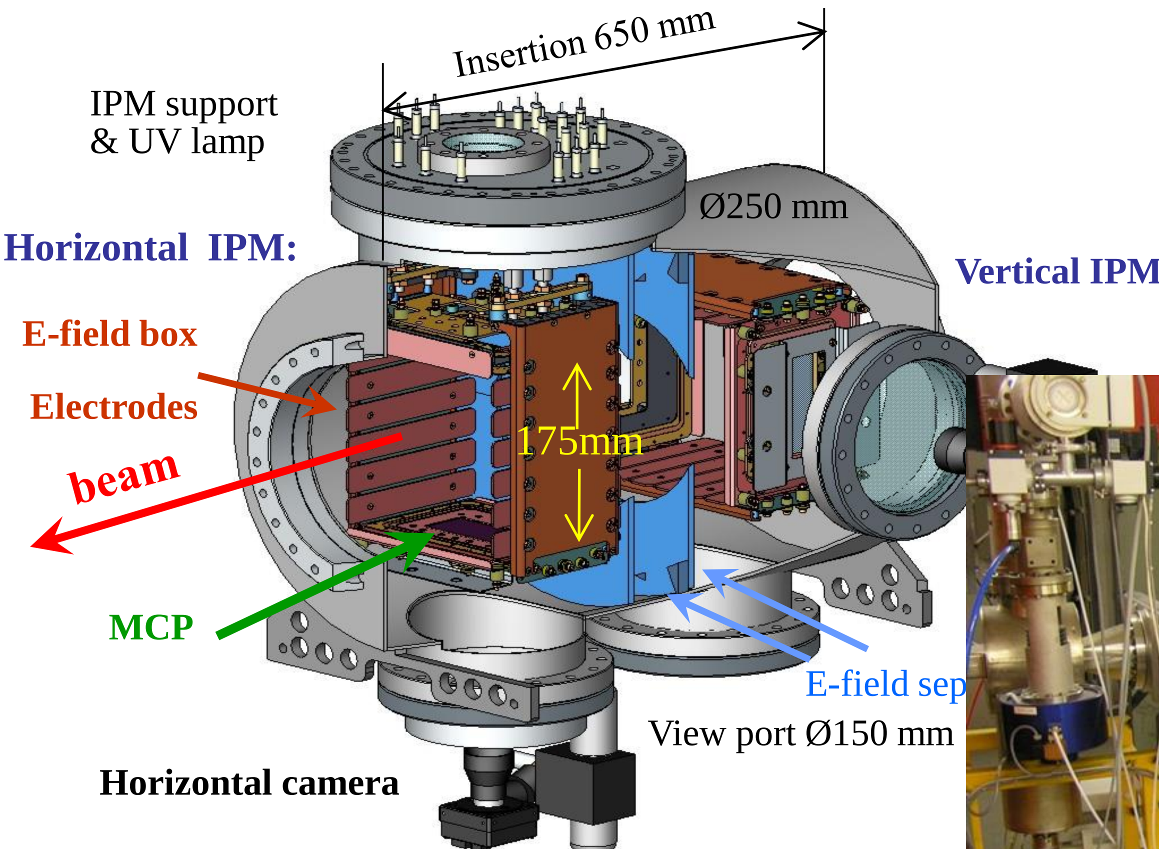

Realization at GSI synchrotron:

Excurse: Multi Channel Plate MCP

MCP are used as particle detectors with secondary electron amplification.

A MCP is:

- 1 mm glass plate with ≈10 μm holes
- thin Cr-Ni layer on surface
- voltage ≈1 kV/plate across

→ e^- amplification of ≈ 10^3 per plate.

→ resolution ≈ 0.1 mm (2 MCPs)

Anode technologies:

- SEM-grid, ≈ 0.5 mm spacing
  → fast electronics readout
- phosphor screen + CCD
  → high resolution, but slow timing
  → fast readout by photo-multipliers
- single particle detection
  → for low beam current.

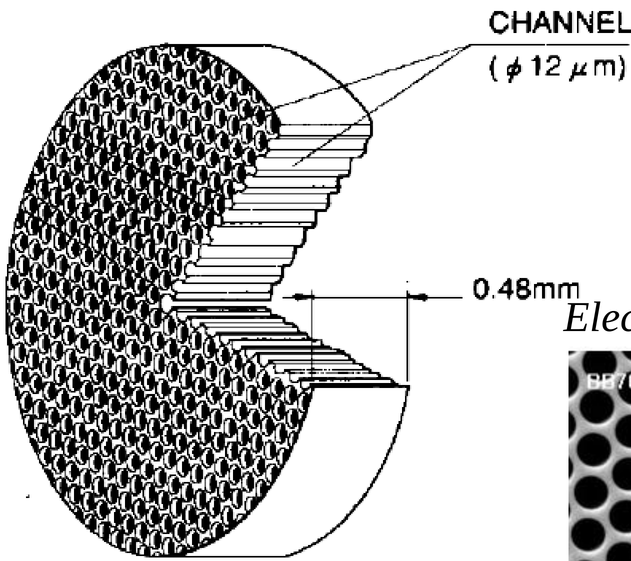

Electron microscope image:

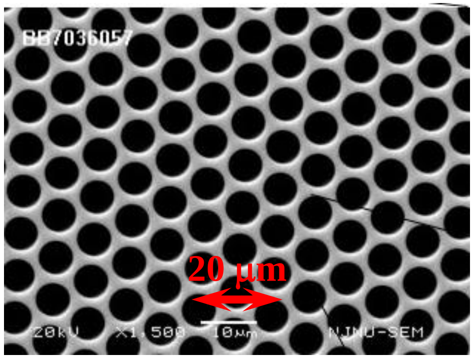

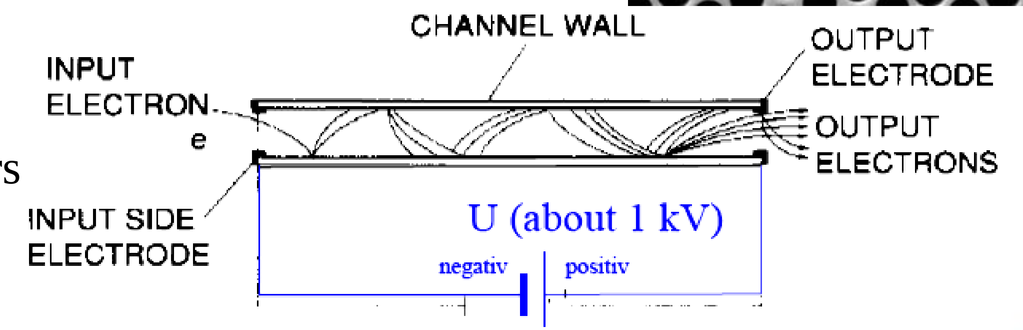

Application: 'Adiabatic' Damping during Acceleration

The emittance $\varepsilon = \int dx dx'$ is defined via the position deviation and angle in **lab-frame**

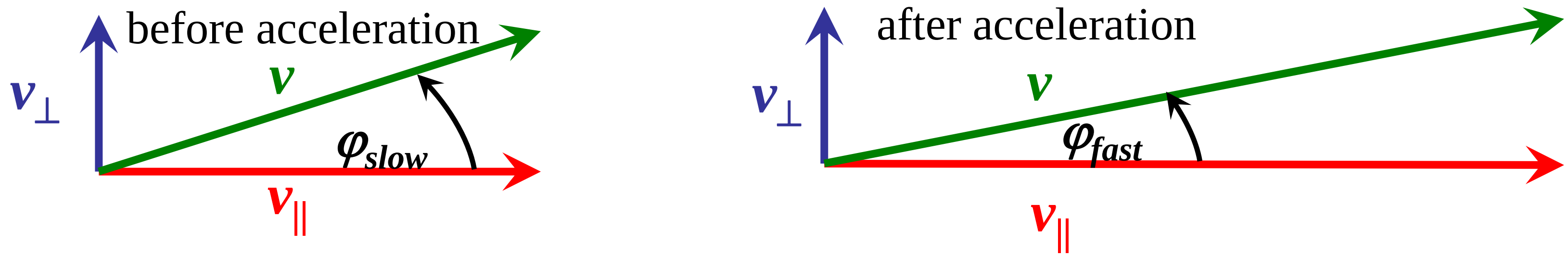

After acceleration the longitudinal velocity is increased $\Rightarrow$ angle $\boldsymbol{\varphi}$ is smaller

The angle is expressed in momenta: $x' = p_\perp / p_\parallel$

the emittance is for $\langle xx' \rangle = 0$: $\varepsilon = x \cdot x' = x \cdot p_\perp / p_\parallel = const.$

$\Rightarrow$ under ideal conditions the emittance can be normalized to the momentum $p_\parallel = \gamma \cdot m \cdot \beta c$

$\Rightarrow$ normalized emittance $\varepsilon_{norm} = \beta\gamma \cdot \varepsilon$ is preserved

with the Lorentz factor $\gamma = (1-\beta^2)^{-1/2}$ and velocity $\beta = v/c$

Example: Acceleration in GSI-synchrotron for C^{6+} from 6.7 $\rightarrow$ 600 MeV/u (β = 12 $\rightarrow$ 79%) observed by IPM

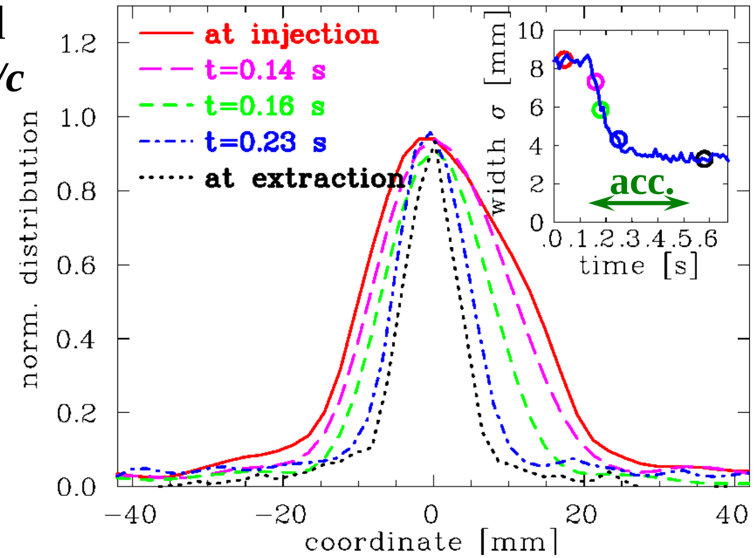

theoretical width: $\langle x \rangle_f = \sqrt{\frac{\beta_i \cdot \gamma_i}{\beta_f \cdot \gamma_f}} \cdot \langle x \rangle_i = 0.33 \cdot \langle x \rangle_i$

measured width: $\langle x \rangle_f \approx 0.37 \cdot \langle x \rangle_i$

Non-intercepting ionization profile monitor is well suited for long time observations without beam disturbance

$\rightarrow$ mainly used at proton synchrotrons.

Influence of the residual gas ion trajectory by :

- External electric field $\boldsymbol{E_{ex}}$
- Electric field of the beam's space charge $\boldsymbol{E_{space}}$

e.g. Gaussian density distribution for round beam: $E_{space}(r) = \frac{1}{2\pi\varepsilon_0} \cdot \frac{qeN}{l} \cdot \frac{1}{r} \cdot \left[1 - \exp\left(-\frac{r^2}{2\sigma^2}\right)\right]$

Estimation of correction: $\sigma_{corr}^2 \approx \frac{e^2 \ln 2}{4\pi\varepsilon_0 \sqrt{m_p c^2}} \cdot \frac{qN}{l} \cdot d_{gap} \cdot \sqrt{\frac{1}{eU_{ex}}} \propto N \cdot d_{gap} \cdot \sqrt{\frac{1}{U_{ex}}}$

With the measured beam width is given by convolution: $\sigma_{meas}^2 = \sigma_{true}^2 + \sigma_{corr}^2$

Example: U^{73+}, 10^9 particles per 3 m bunch length, cooled beam with $\boldsymbol{\sigma_{true}}$ = 1 mm FWHM.

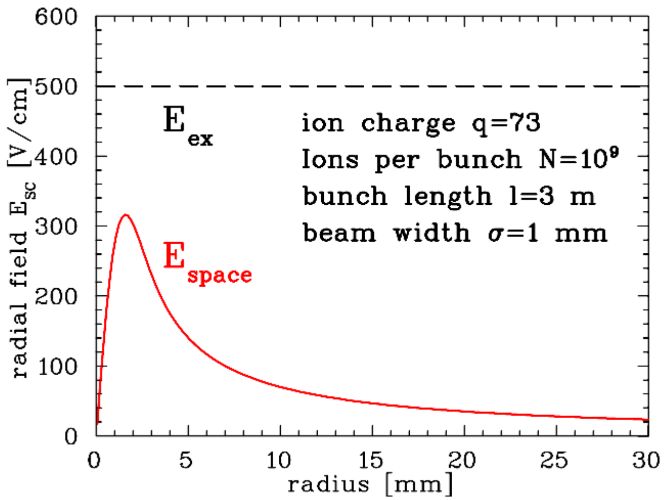

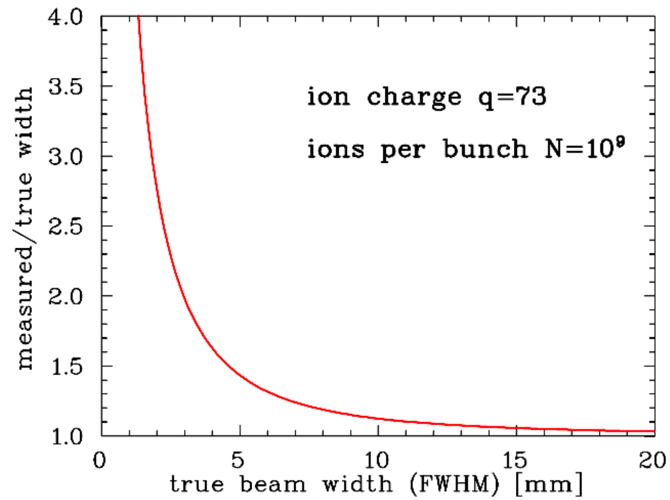

Alternative: e^- detection in an external magnetic field

$\rightarrow$ cyclotron radius $r_c = \sqrt{2m_e E_{kin,\perp}}/eB \Rightarrow r_c < 0.1\,\text{mm}$ for $B = 0.1\,\text{T}$

E_{kin}, given by atomic physics, 0.1 mm is internal resolution of MCP.

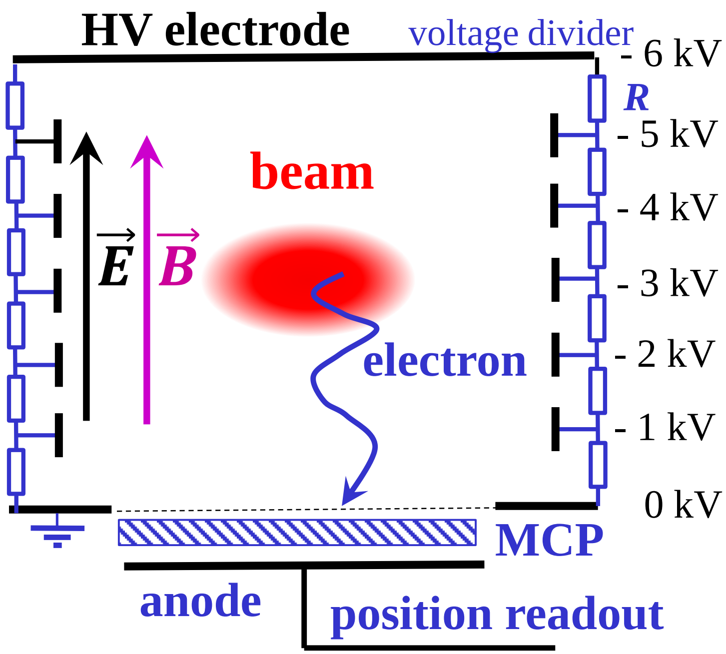

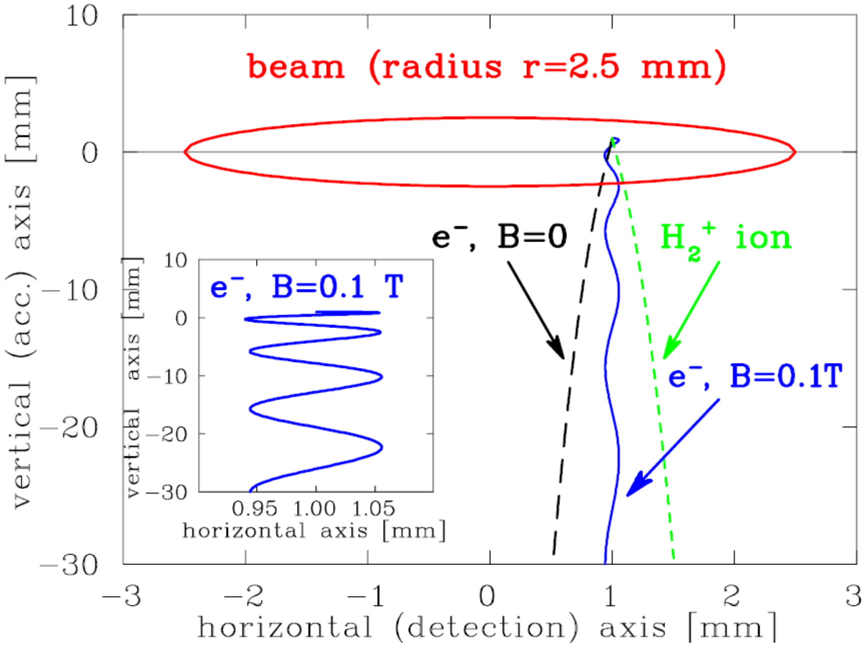

Time-of-flight: ≈1 ns → 2 or 3 cycles.

B-field: By dipole magnets with large aperture → IPM is expensive device.

Magnetic field for electron guidance:

Maximum image distortion:

5% of beam width ⇒ $\Delta B/B < 1\ \%$

Challenges:

- High ***B***-field homogeneity of 1%
- Clearance up to 500 mm
- Correctors required
  to compensate beam steering
- Insertion length 2.5 m incl. correctors

For MCP wire-array readout
lower clearance required

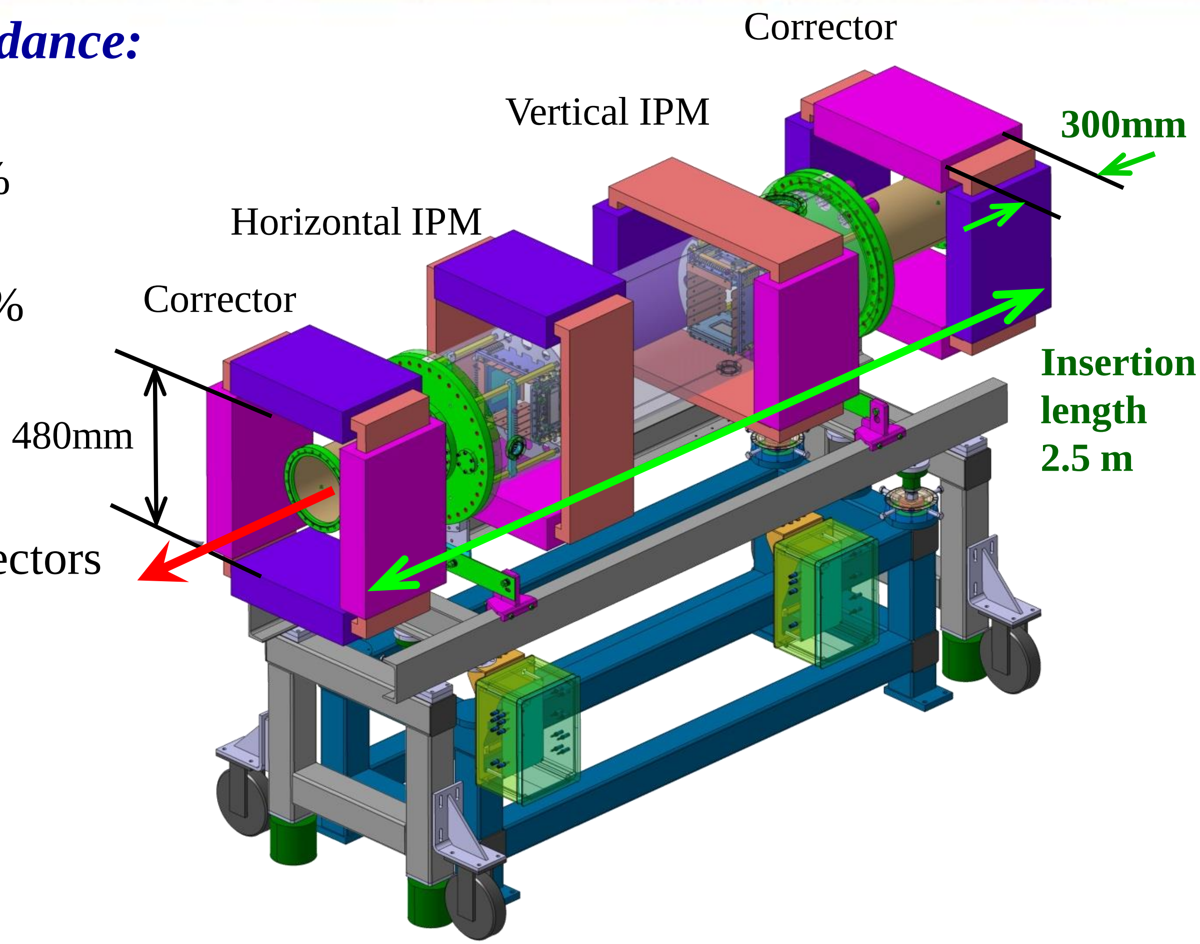

Magnetic field for electron guidance:

Maximum image distortion:

5% of beam width ⇒ $\Delta B / B <$ 1 %

Challenges:

- High ***B***-field homogeneity of 1%
- Clearance up to 500 mm
- Correctors required
  to compensate beam steering
- Insertion length 2.5 m incl. correctors

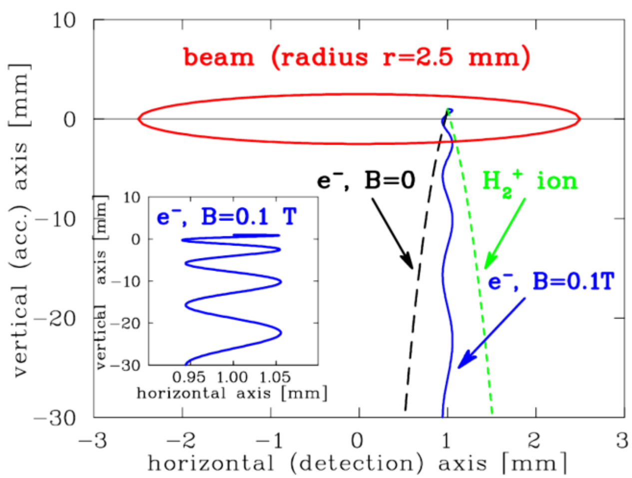

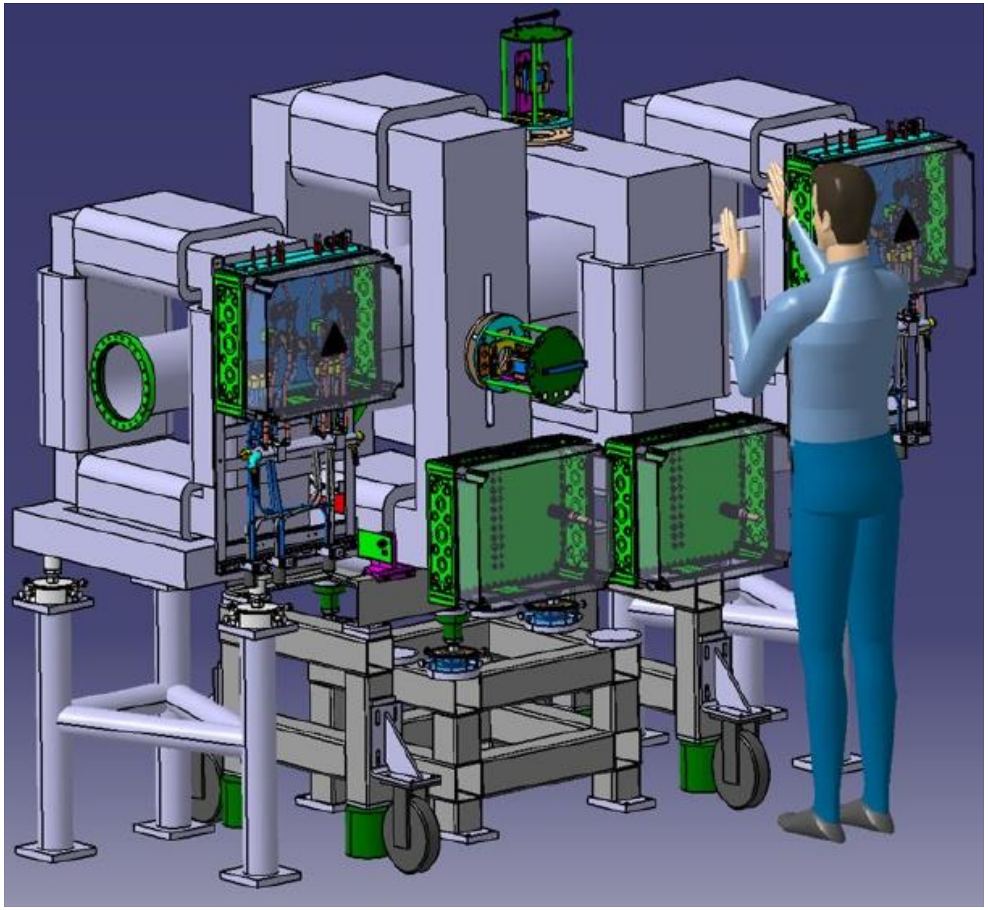

Remark: For MCP wire-array readout lower clearance required

Large beam power → Non-intercepting method:
⇒ **B**eam **I**nduced **F**luorescence BIF
$N_2 + Ion \rightarrow (N_2^{+})^{*} + Ion \rightarrow N_2^{+} + \gamma + Ion$
With single photon detection scheme
390 nm< λ< 470 nm
⇒ non-destructive, compact installation.

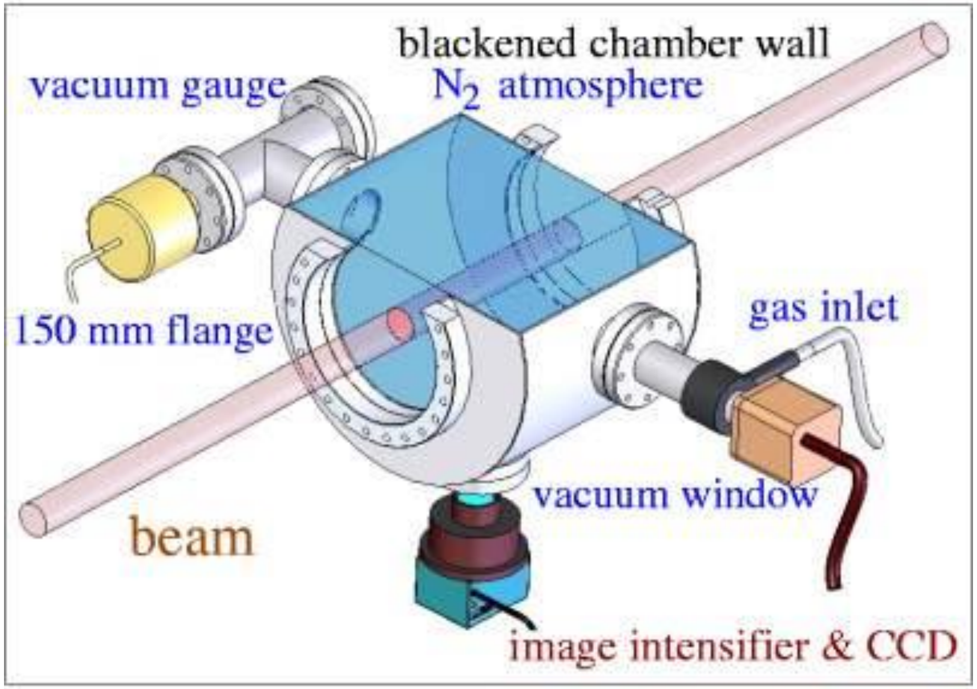

Installation of hor&vert. BIF Monitor:

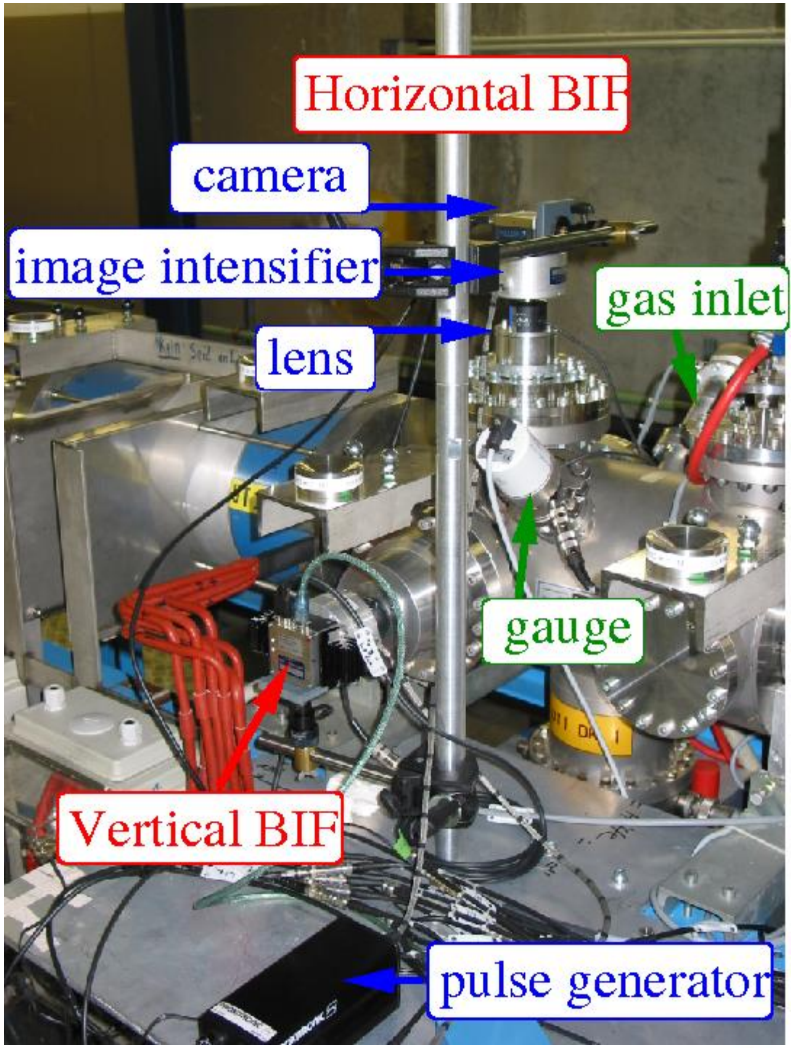

Beam Induced Fluorescence Monitor BIF: Image Intensifier

Scheme of Image intensifier:

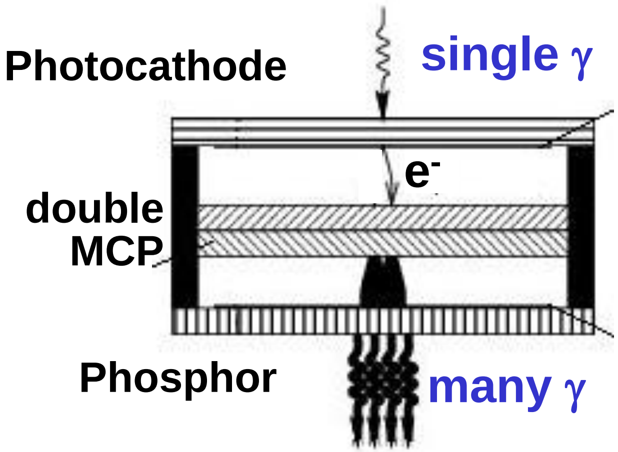

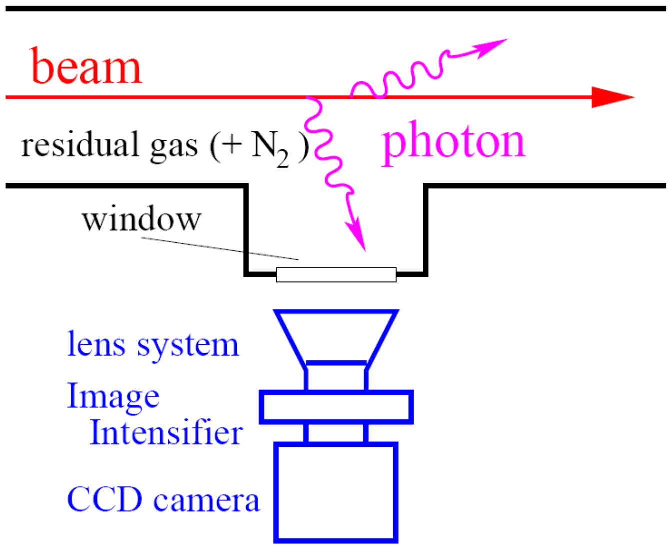

Image intensifier:

- Photo cathode → creation of photo-e⁻
- Accelerated toward MCP for amplification
- Detection of ampl. e⁻ by phosphor screen
- Image recorded by CCD

⇒ Low light amplification
(commercially used for night vision devices)

A BIF monitor consists of only:

- optics outside beam pipe
- image intensifier + camera
- gas-inlet for pressure increase

⇒ nearly no installation inside vacuum.
only LEDs for calibration

⇒ cheaper than IPM, but lower signal.

'Single photon counting':

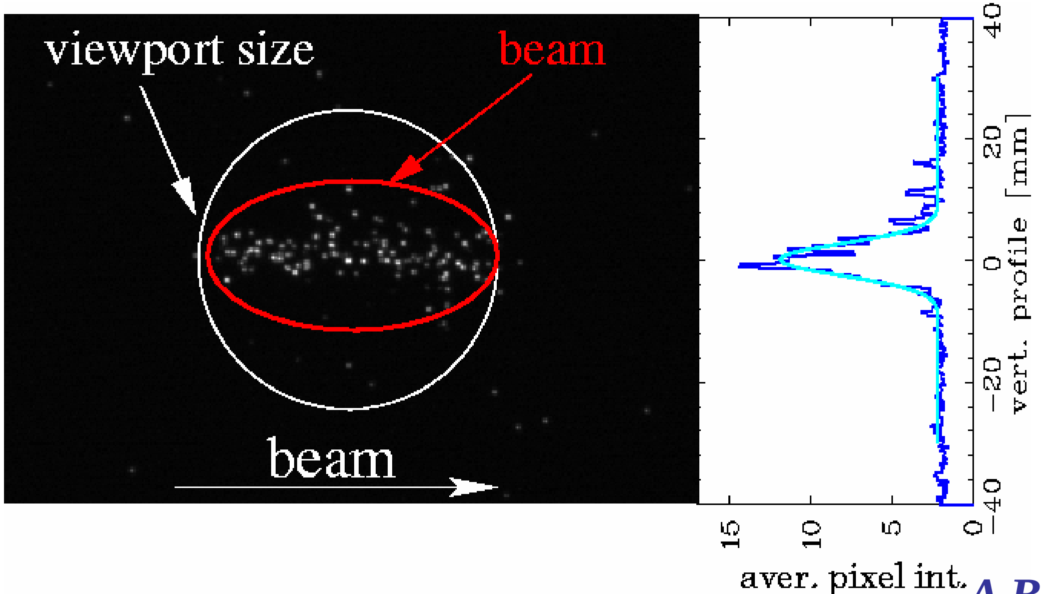

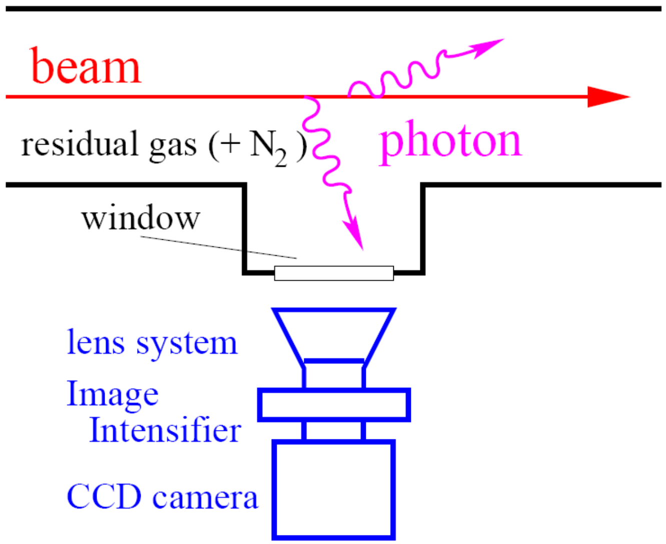

Example at GSI-LINAC:

4.7 MeV/u Ar $^{10+}$ beam

I=2.5 mA equals to 10^{11} particle

One single macro pulse of 200 μs

Vacuum pressure: p=10^{-5} mbar (N_2)

A BIF monitor consists of only:

- optics outside beam pipe
- image intensifier + camera
- gas-inlet for pressure increase

⇒ nearly no installation inside vacuum.
only LEDs for calibration

⇒ cheaper than IPM, but lower signal.

Comparison between IPM and BIF

Non-destructive methods preferred:

Beam is not influenced and diagnostics device is not destroyed!

IPM: Beam ionizes the residual gas
$\rightarrow$ measurement of all ionization products, $\boldsymbol{\Omega = 4\pi}$-geometry due to E-field

BIF: Beam ionizes and excites the residual gas
$\rightarrow$ measurement of photons emitted toward camera, solid angle $\boldsymbol{\Omega \approx 10^{-3}}$

IPM: Higher efficiency than BIF

BIF: Low detection efficiency, only $\approx 10^{-4}$ of IPM
$\Rightarrow$ longer observation time or higher pressure required

---

IPM: Complex installation inside vacuum

BIF: Nearly no installation inside vacuum

IPM: More expensive, for some beam parameters even guiding magnetic field required

BIF: More sensitive to external parameters like radiation stray light

Outline:

- Scintillation screens:
  emission of light. universal usage, limited dynamic range
- SEM-Grid: emission of electrons, workhorse, limited resolution
- Wire scanner: emission of electrons, workhorse, scanning method
- Ionization Profile Monitor and Beam Induced Fluorescence Monitor:
  secondary particle detection from interaction beam-residual gas
- **Optical Transition Radiation:**
  crossing material boundary, for relativistic beams only
- Synchrotron Light Monitors
- Summary

Optical Transition Radiation OTR for a single charge *e*:

Assuming a charge ***e*** approaches an ideal conducting boundary e.g. metal foil

- image charge is created by electric field
- dipole type field pattern
- field distribution depends on velocity β and Lorentz factor γ due to relativistic trans. field increase
- penetration of charge through surface within t < 10 fs: sudden change of source distribution
- emission of radiation with dipole characteristic

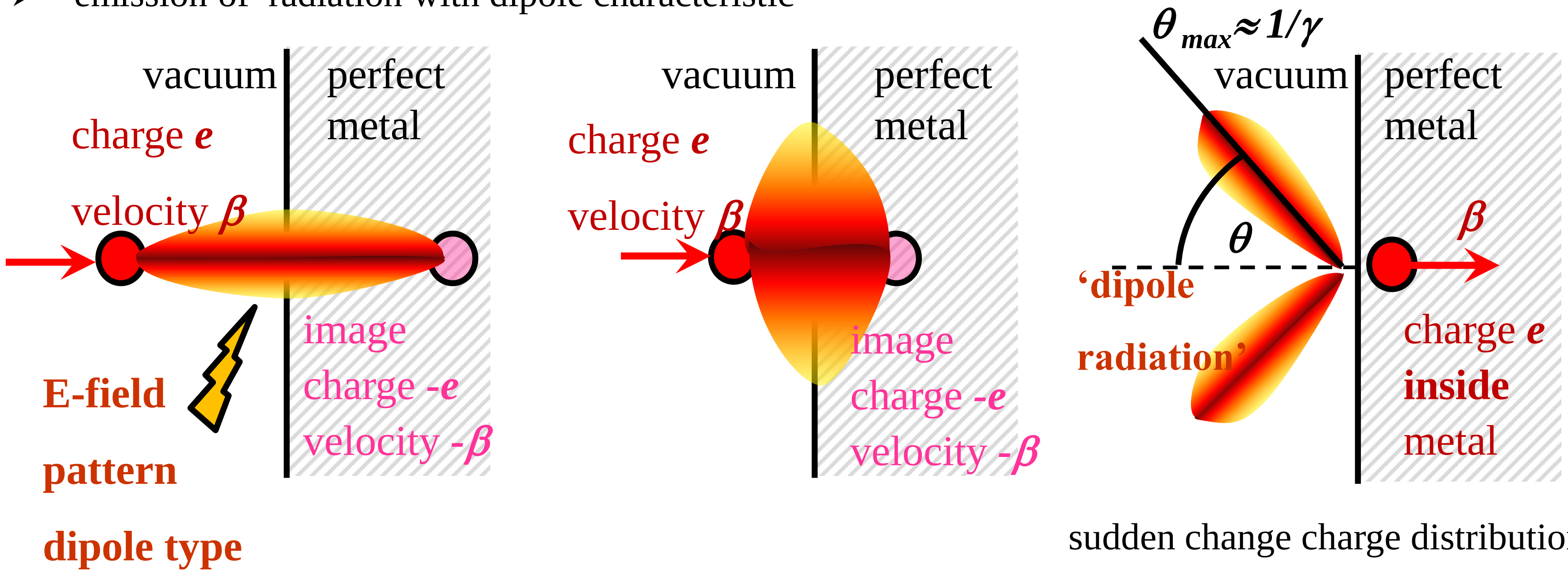

sudden change charge distribution
rearrangement of sources ⇔ radiation

Other physical interpretation: Impedance mismatch at boundary leads to radiation

Excurse: Optical Transition Radiation: Depictive Description

Optical Transition Radiation OTR can be described in classical physics:

approximated formula for normal incidence & in plane polarization:

$$\frac{d^2W}{d\theta\, d\omega} \approx \frac{2e^2\beta^2}{\pi c} \cdot \frac{\sin^2\theta \cdot \cos^2\theta}{\left(1-\beta^2\cos^2\theta\right)^2}$$

W: radiated energy

ω: frequency of wave

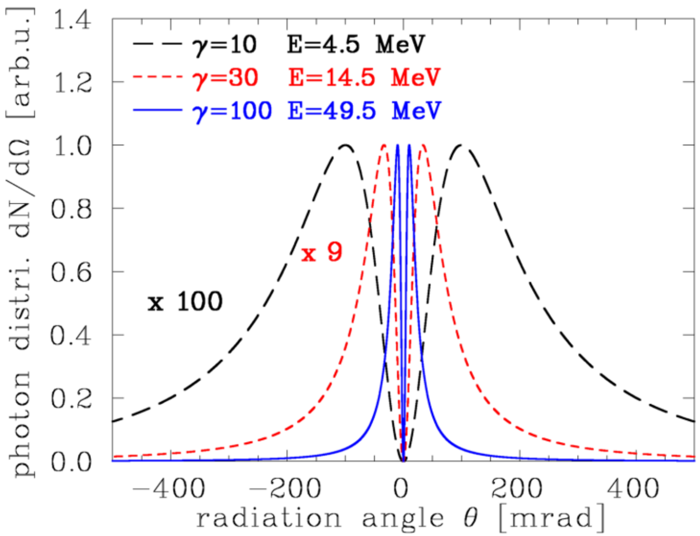

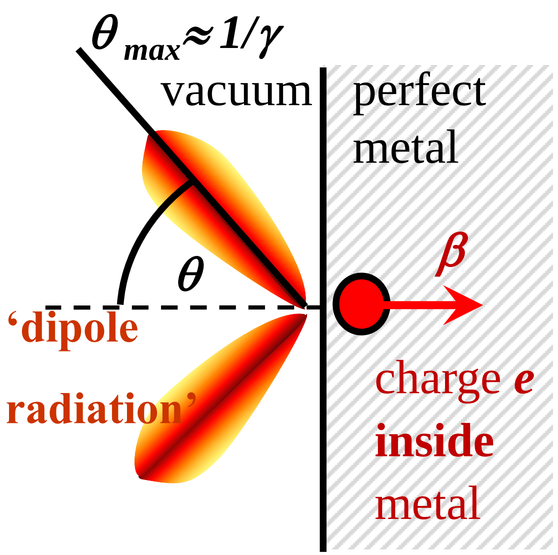

Angular distribution of radiation in optical spectrum:

- lope emission pattern depends on velocity or Lorentz factor γ
- peak at angle $\theta \approx 1/\gamma$
- emitted energy i.e. amount of photons scales with $W \propto \beta^2$
- broad wave length spectrum (i.e. no dependence on ω)

→ suited for high energy electrons

sudden change charge distribution
rearrangement of sources ⇔ radiation

OTR with 45⁰ beam incidence and observation at 90⁰ :

A charge ***e*** approaches an ideal conducting boundary under 45^0

- image charge is created by electric field
- dipole rotated by 45^0 & deformed due to relativistic field propagation
- penetration of surface within ***t*** < 10 fs: sudden change of sources
- due to reflection on surface emission symmetric around 90^0

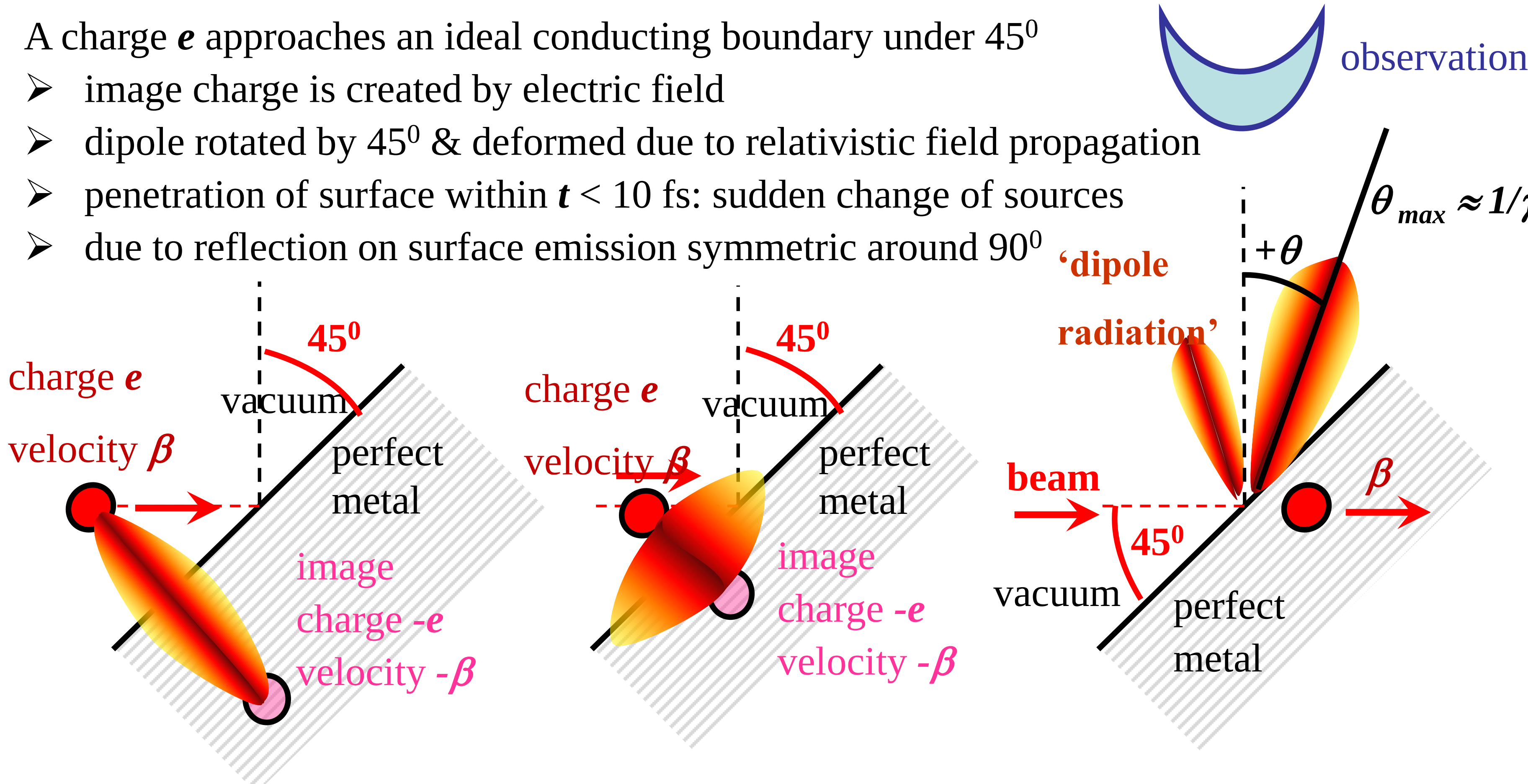

OTR with 45⁰ beam incidence and observation at 90⁰ :

approximated formula for 45⁰ incidence& in plane polarization:

$$\frac{d^2W}{d\theta\, d\omega} \approx \frac{2e^2\beta^2}{\pi\, c}\cdot\left(\frac{\sin\theta}{1-\beta\cos\theta}+\frac{\cos\theta}{1-\beta\sin\theta}\right)^2$$

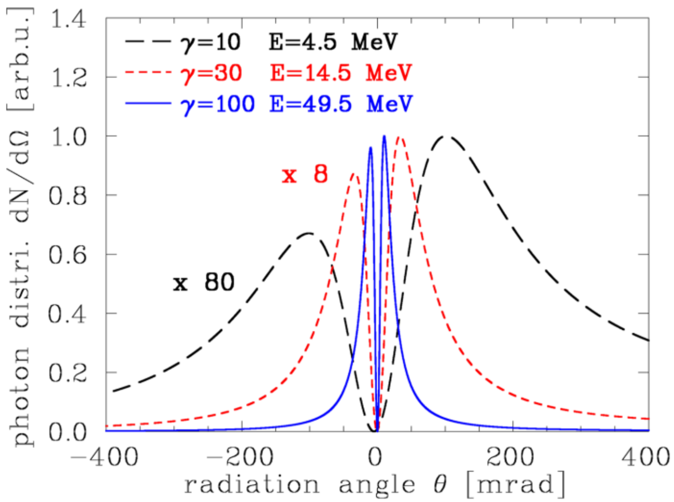

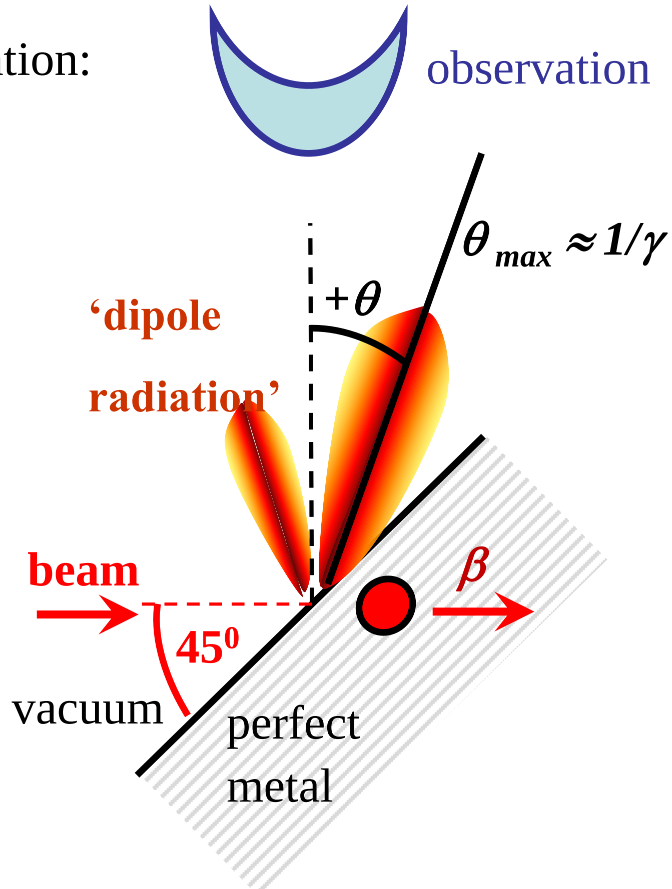

Angular distribution of radiation in optical spectrum:

- emission pattern depends on velocity
- peak at angle $\theta \approx 1/\gamma$
- emitted energy scales with $W \propto \beta^2$
- symmetric with respect to θ for γ > 100

Remark: polarization of emitted light:

- in scattering plane → parallel E-vector
- perpendicular plane → rectangular E-vector

Optical transition radiation is emitted by charged particle passage through a material boundary.

Electrodynamics field configuration changes during the passage:
$\rightarrow$ Polarization of the medium
$\rightarrow$ emission of energy
Description by
classical electrodynamics & relativity:

$$\frac{d^2W}{d\Omega d\omega} \approx \frac{2e^2\beta^2}{\pi c} \cdot \frac{\theta^2}{\left(\gamma^{-2} + \theta^2\right)^2}$$

W: energy emitted in solid angle Ω
θ: angle of emission
γ: Lorentz factor
ω: angular frequency intervall $E_{ph}=2\pi h\omega$

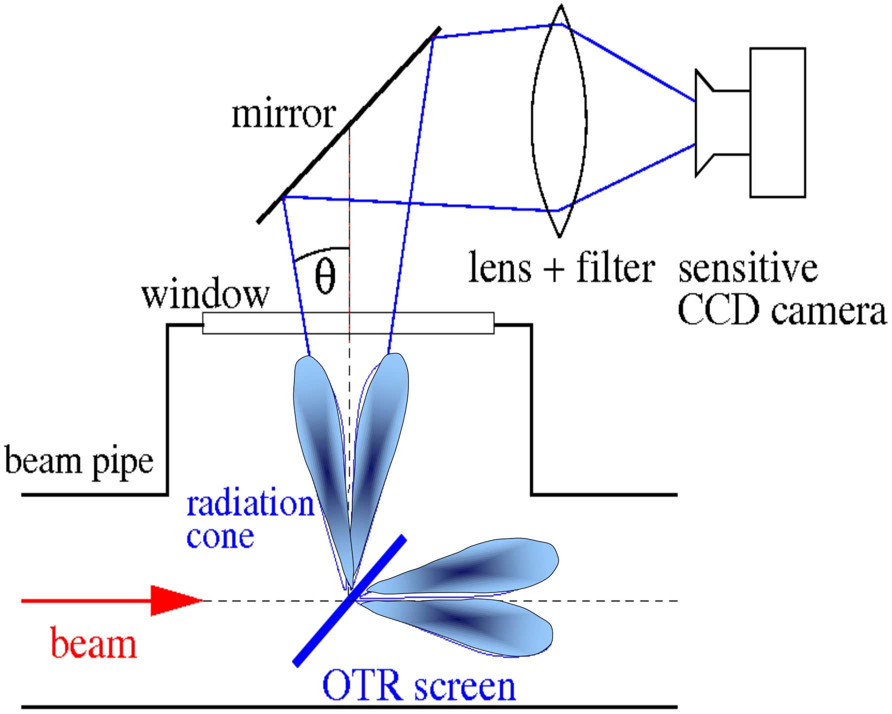

- Insertion of thin Al-foil under 45°
- Observation of low light by CCD.

Optical Transition Radiation: Angular Photon Distribution

Photon distribution within a solid angle $d\Omega$ and Wavelength interval λ_{begin} to λ_{end}

$$\frac{dN_{photon}}{d\Omega} = N_{beam} \cdot \frac{2e^2\beta^2}{\pi c} \cdot \log\left(\frac{\lambda_{begin}}{\lambda_{end}}\right) \cdot \frac{\theta^2}{\left(\gamma^{-2}+\theta^2\right)^2}$$

- Detection: Optical 400 nm < λ < 800 nm
  using image intensified CCD
- Larger signal for relativistic beam γ >> 1
- Angular focusing for γ >> 1

⇒ **well suited for e⁻ beams**

⇒ **p-beam only for E_{kin}>10 GeV (γ>10)**

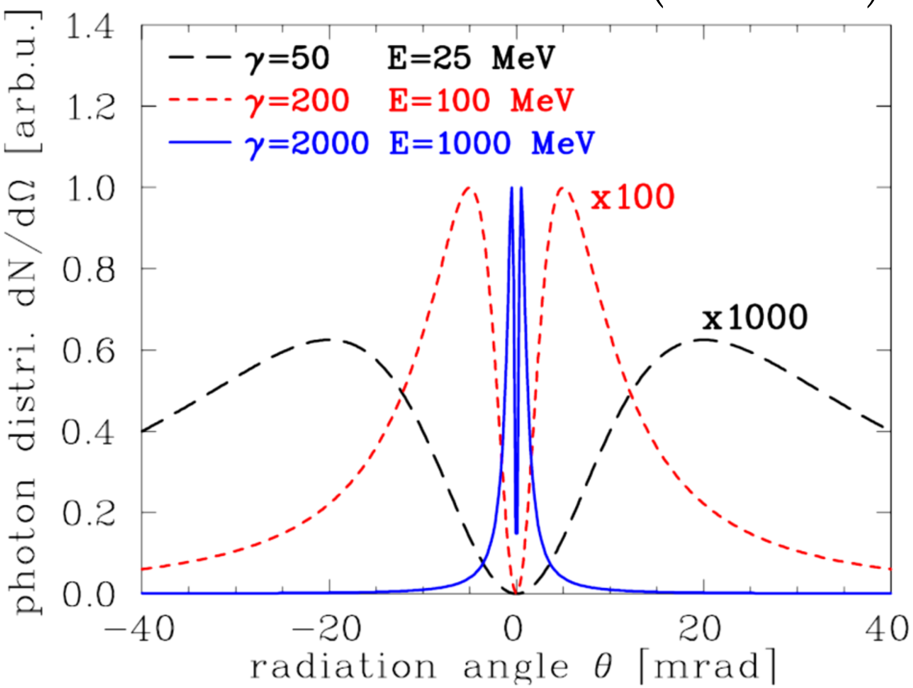

Remark:

→ ***Profile*** by focusing to screen

→ ***Beam angular distribution*** by focusing on infinity due to emission dependence on beam angular distribution.

OTR-Monitor: Technical Realization and Results

Example of realization at TERATRON:

- Insertion of foil
  e.g. 5 μm Kapton coated with 0.1μm Al

Advantage: thin foil ⇒ low heating & straggling
2-dim image visible

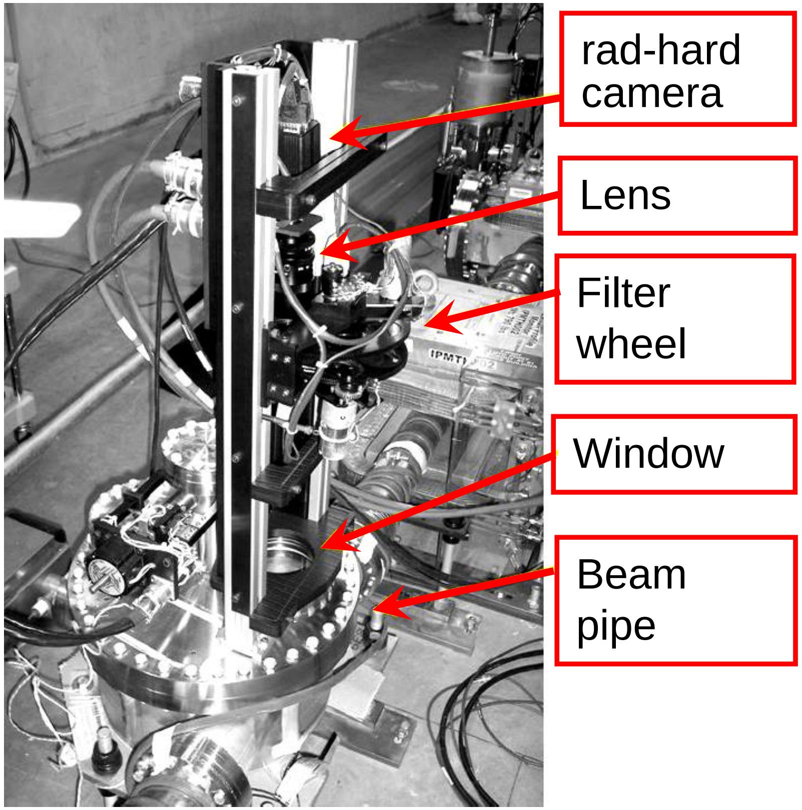

Results at FNAL-TEVATRON synchrotron with 150 GeV proton
Using fast camera: Turn-by-turn measurement

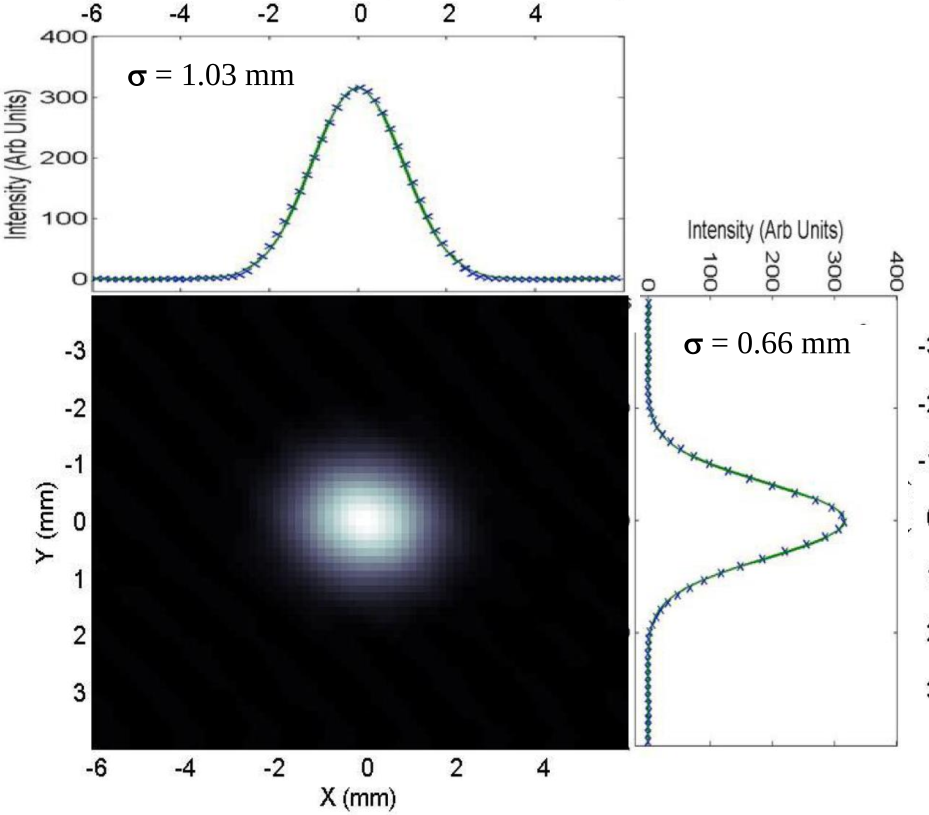

From V.E. Scarpine (FNAL) et al., BIW'06

Installation of OTR and scintillation screens on same drive :

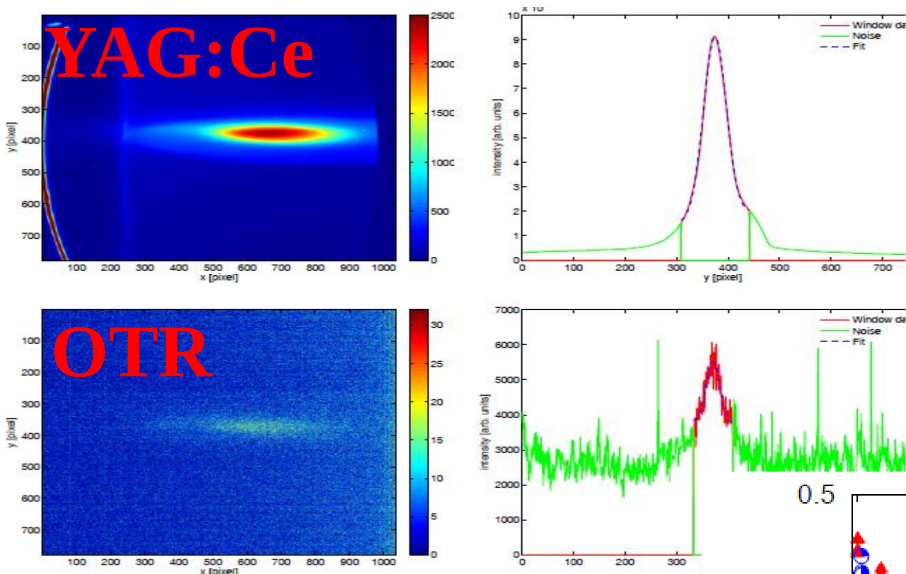

Example: ALBA LINAC 100 MeV

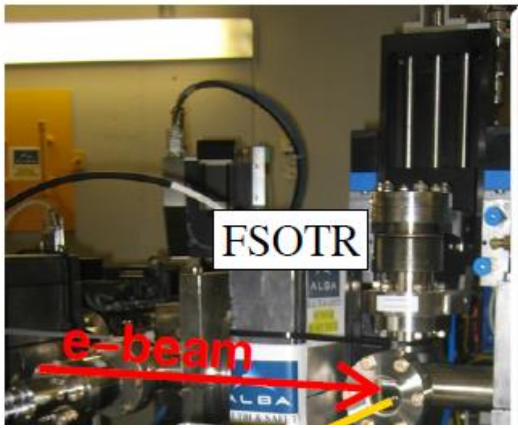

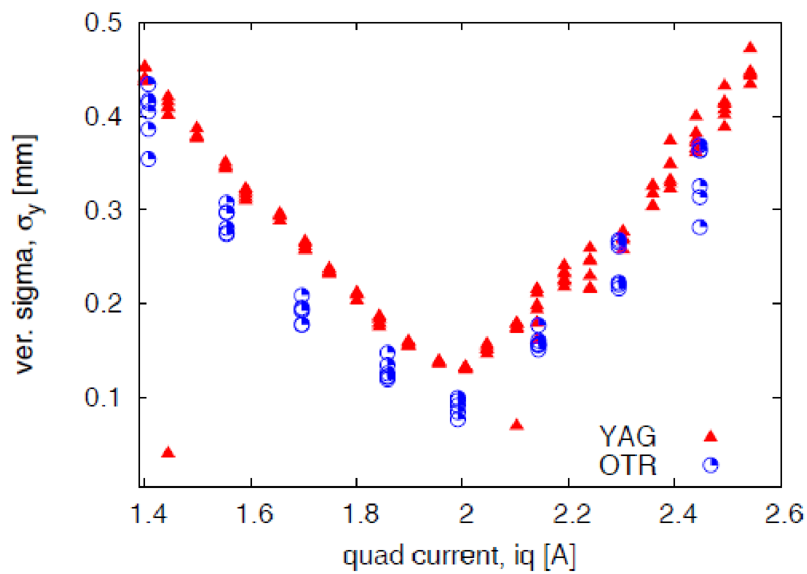

Results:

- Much more light from YAG:Ce for 100 MeV (γ=200) electrons light output $I_{YAG} \approx 10^5 \, I_{OTR}$
- Broader image from YAG:Ce due to finite shoulders or CCD saturation(?)

Contrary of U. Iriso et al., DIPAC'09

Comparison between Scintillation Screens and OTR

OTR: electrodynamic process → beam intensity linear to # photons

Scint. Screen: complex atomic process → saturation possible

OTR: thin foil Al or Al on Mylar, down to 0.25 μm thickness

→ minimization of beam scattering (Al is low Z-material)

Scint. Screen: thickness ≈ 1 mm inorganic, fragile material, not radiation hard

---

OTR: low number of photons → expensive image intensified CCD

Scint. Screen: large number of photons → simple CCD sufficient

---

OTR: complex angular photon distribution → resolution limited

Scint. Screen: isotropic photon distribution → simple interpretation

---

OTR: beam angular distribution measurable→ beam emittance

Scint. Screen: no information concerning the beam angular distribution

---

OTR: large γ needed → e^--beam with $E_{kin} > 100$ MeV, proton-beam with $E_{kin} > 100$ GeV

Scint. Screen: for all beams

Outline:

- **Scintillation screens:**
  emission of light, universal usage, limited dynamic range
- **SEM-Grid: emission of electrons, workhorse, limited resolution**
- **Wire scanner: emission of electrons, workhorse, scanning method**
- **Ionization Profile Monitor and Beam Induced Fluorescence Monitor:**
  secondary particle detection from interaction beam-residual gas
- **Optical Transition Radiation:**
  crossing optical boundary, for relativistic beams only
- **Synchrotron Light Monitors**
  photon detection of emitted synchrotron light in optical and x-ray range
- **Summary**

An electron bent (i.e. accelerated) by a dipole magnet emit synchrotron light.

This light is emitted
into a cone of
opening $2/\gamma$ in lab-frame.
$\Rightarrow$Well suited for rel. e^-
For protons:
Only for energies E_{kin} > 100 GeV

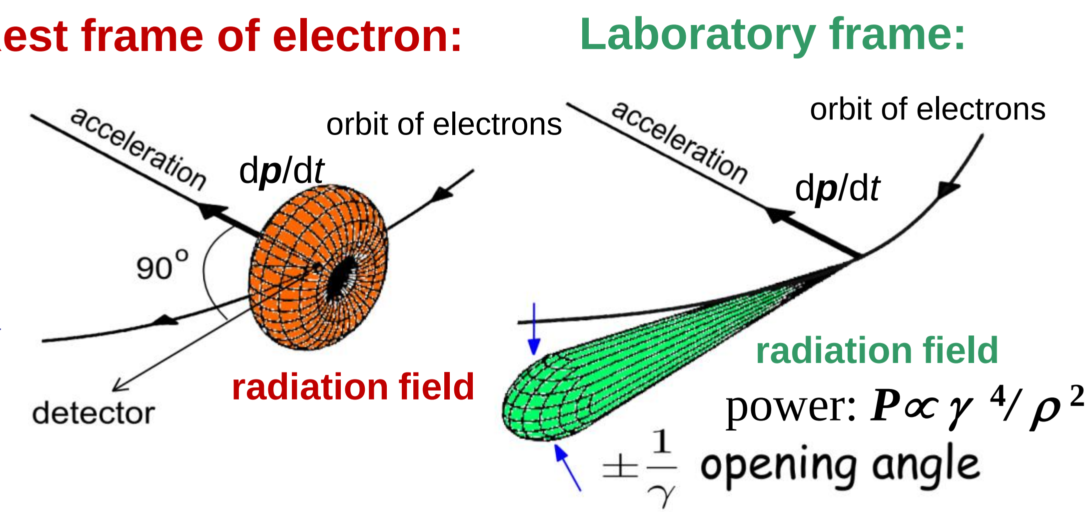

The light is focused to a
intensified CCD.

Advantage:
Signal anyhow available!

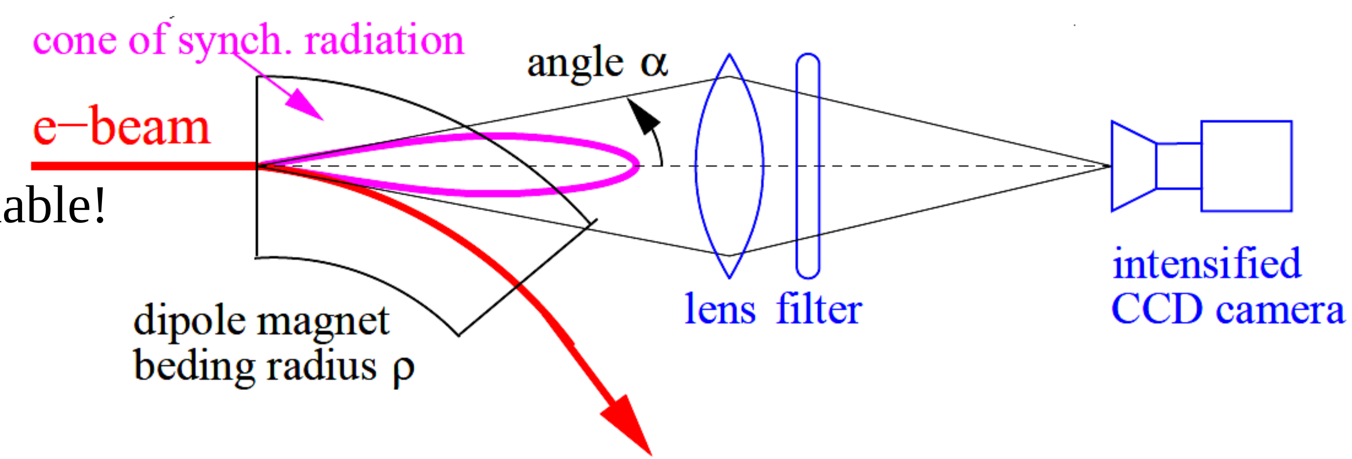

Realization of a Synchrotron Light Monitor

Extracting out of the beam's plane by a (cooled) mirror
→ Focus to a slit + wavelength filter for optical wavelength
→ Image intensified CCD camera

Example: CERN LEP-monitor with bending radius 3.1 km (blue or near UV)

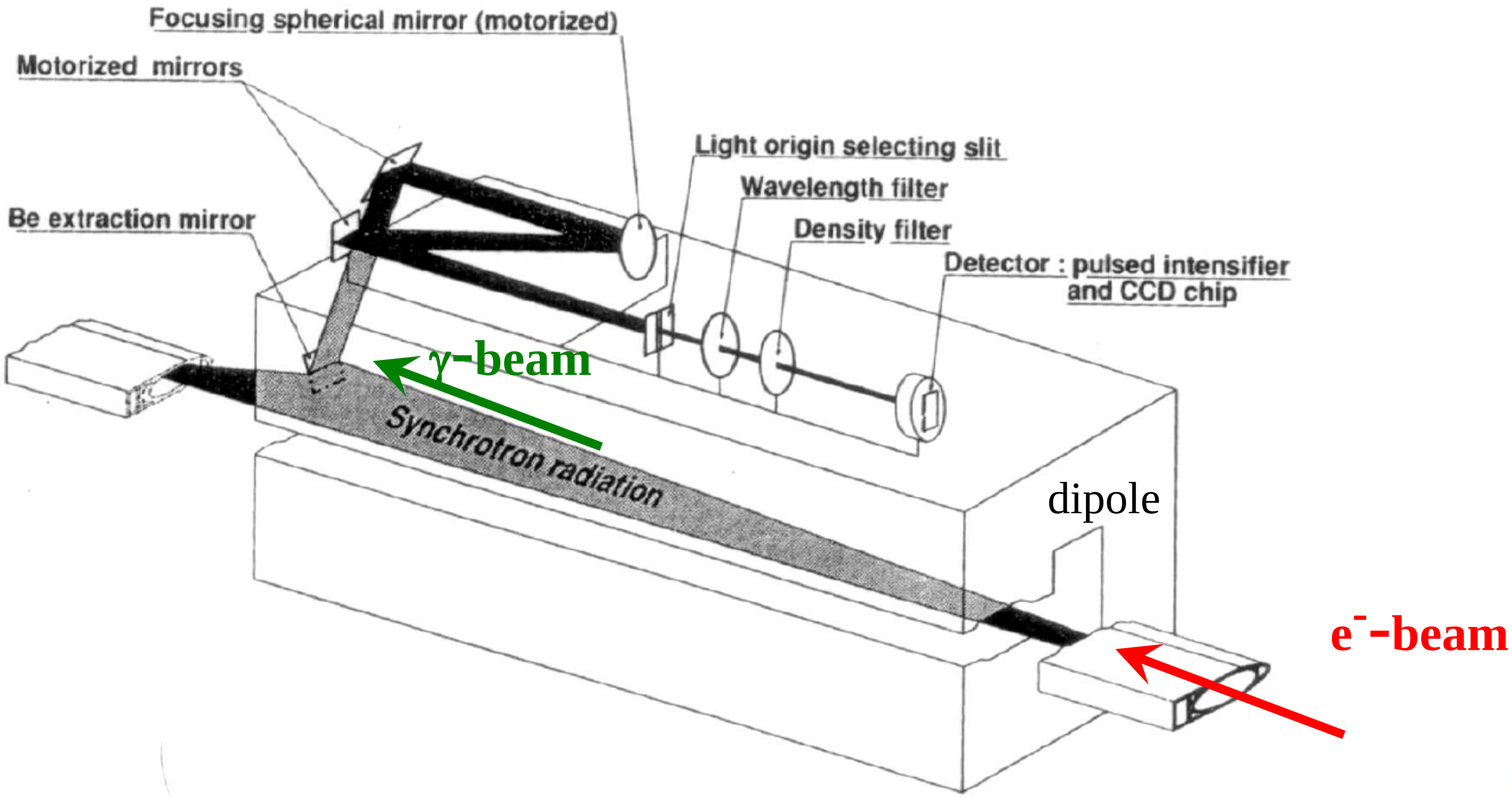

Result from a Synchrotron Light Monitor

Example: Synchrotron radiation facility APS accumulator ring and blue wavelength:

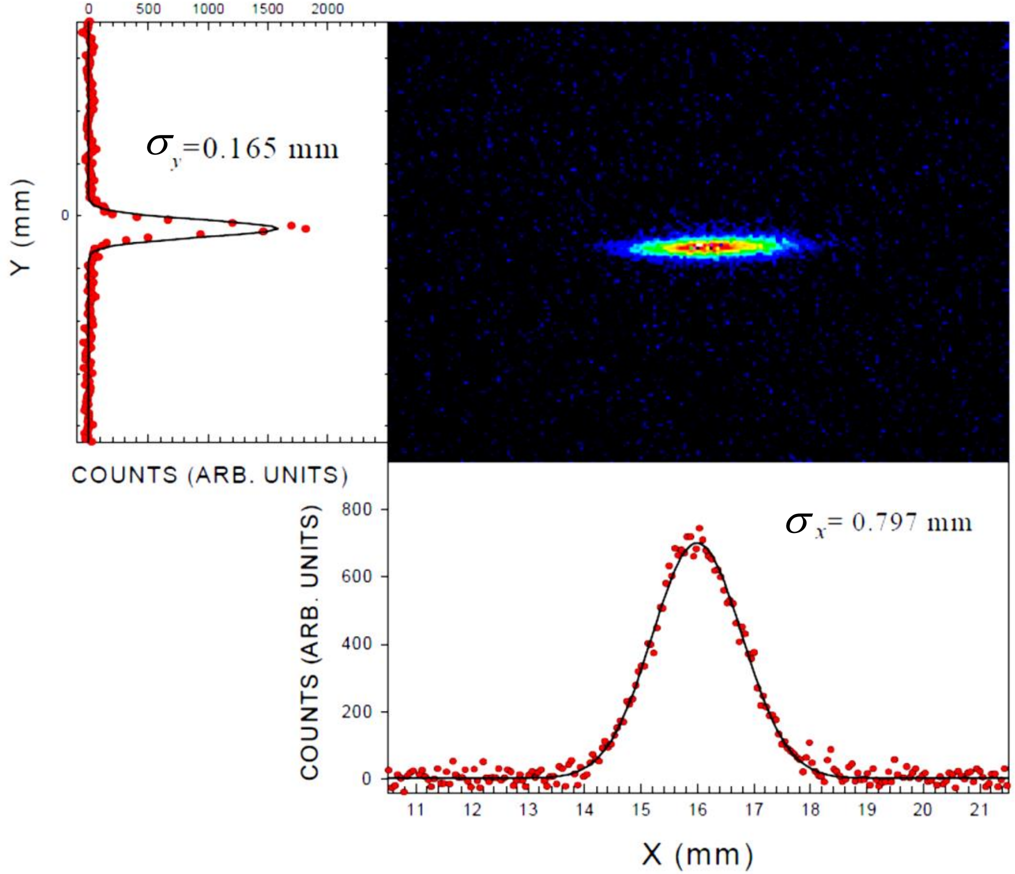

Advantage: Direct measurement of 2-dim distribution, only mirror installed in the vacuum pipe

Realization: Optics outside of vacuum pipe

Disadvantage: Resolution limited by the diffraction due to finite apertures in the optics.

The Artist View of a Synchrotron Light Monitor

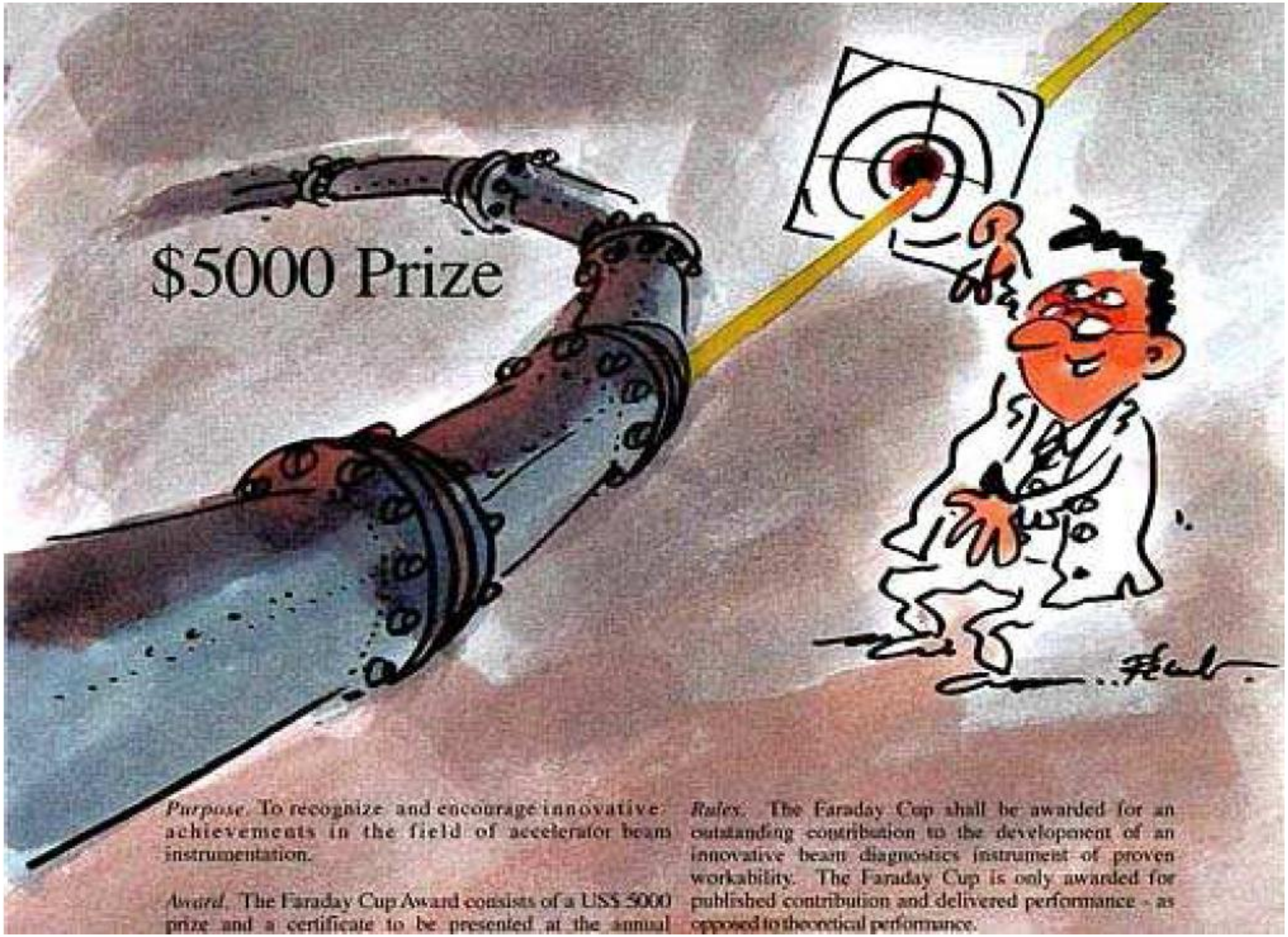

Diffraction Limit for a Synchrotron Light Monitor

Use of optical wavelength and CCD: λ above critical λ_{crit} (spectrum fall-off).

Example 1:1 image: Cone of emission for horizontally polarized light: $\alpha = 0.41\ (\lambda/\rho)^{1/3}$

General Fraunhofer diffraction limit (given by emission cone): $\sigma = \dfrac{\lambda}{2D/L}$

Opening angle of optics: $D = 2\alpha \cdot L$

Diffraction pattern with $\Rightarrow \sigma \cong 0.6 \cdot \left(\lambda^2/\rho\right)^{1/3}$

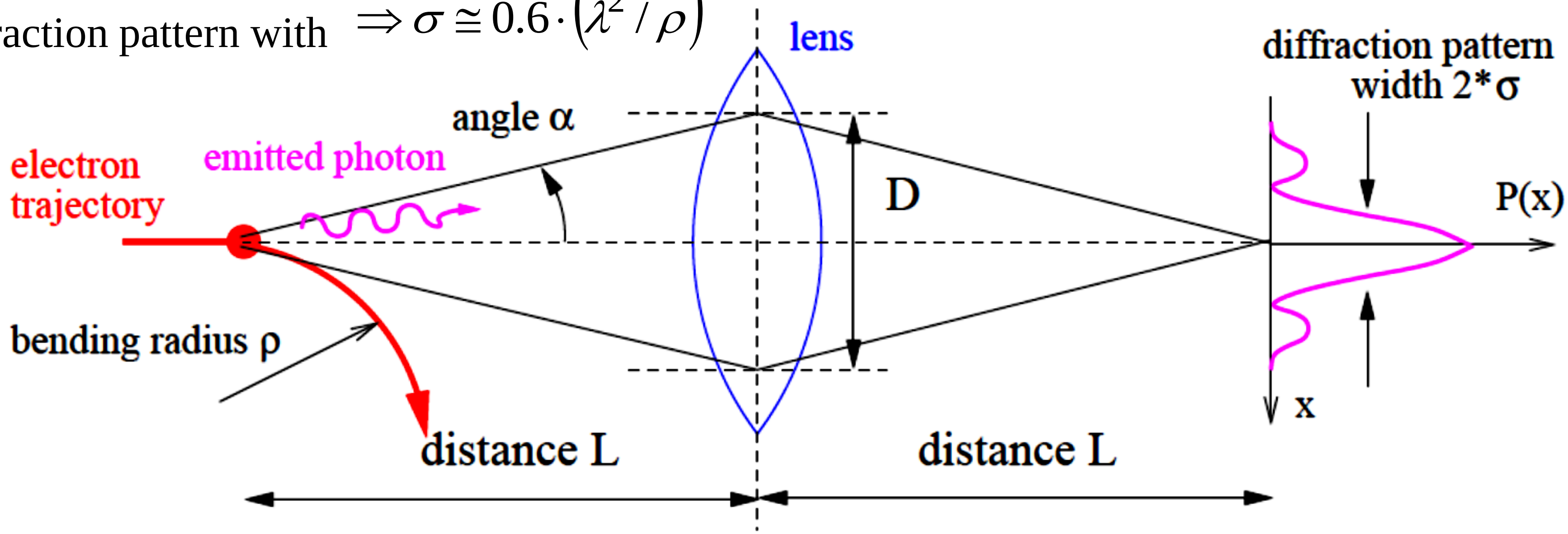

A good resolution for:

- large dipole bending radius ρ, **but** fixed by the accelerator
- short wavelength, **but** good optics only for $\lambda > 300$ nm

The resolution is limited by:

- Fraunhofer diffraction due to finite emission cone and finite size of optics
- Depth of field
- Spectral width of observed light → usage of interference filters
- Time variation of light due to finite observation angle → usage of aperture
- Light intensity and related noise → usage of sensitive CCD camera

⇒ typical value for resolution $\boldsymbol{\sigma \approx 100}$ **µm**

→ which is comparable to the electron beam size of **modern** 3rd generation light source

Scheme for time variation:

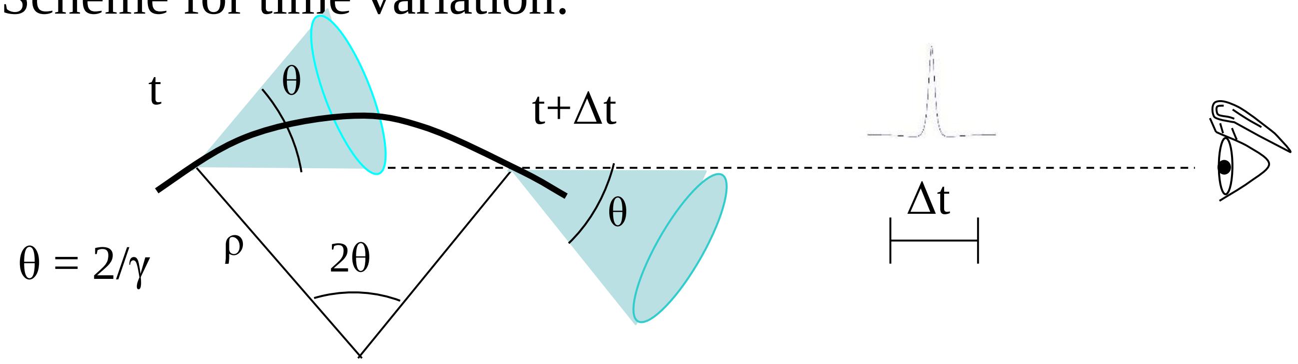

$$\Delta t = \frac{4\rho}{3\gamma^3 c}$$

Courtesy of G. Kube DESY

The diffraction limit is $\Rightarrow \sigma \cong 0.6 \cdot \left(\lambda^2 / \rho\right)^{1/3} \approx 100$ μm for typical case

Possible improvements:

- ***Shorter wavelength:*** Using x-rays and an aperture of Ø 1mm
  → 'x-ray pin hole camera', achievable resolution $\sigma \approx 10$ μm
- ***Interference technique:*** At optical wavelength using a double slit
  → interference fringes leading to a resolution $\sigma \approx 1$ μm.

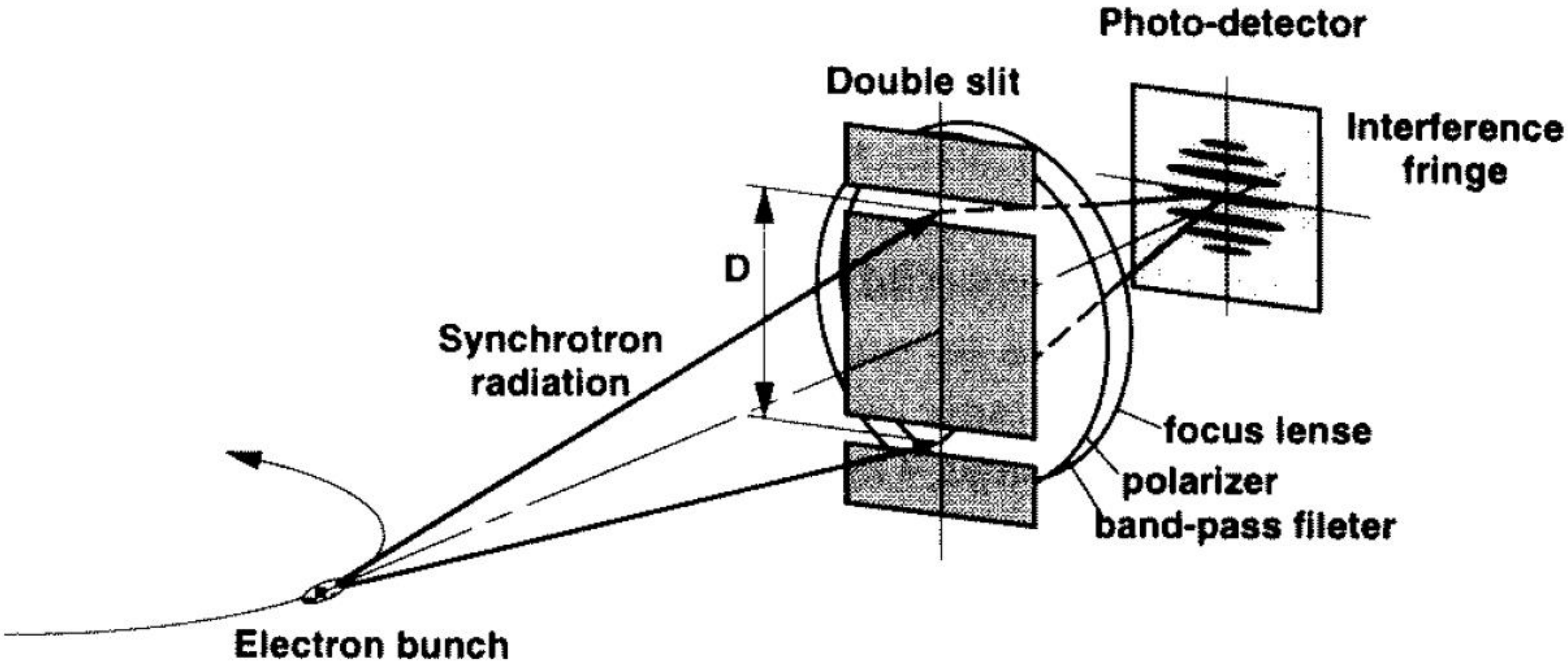

The diffraction limit is $\Rightarrow \sigma \cong 0.6 \cdot \left(\lambda^2 / \rho\right)^{1/3}$ $\Rightarrow$ s***horter wavelength by x-rays***.

Example: PETRA III

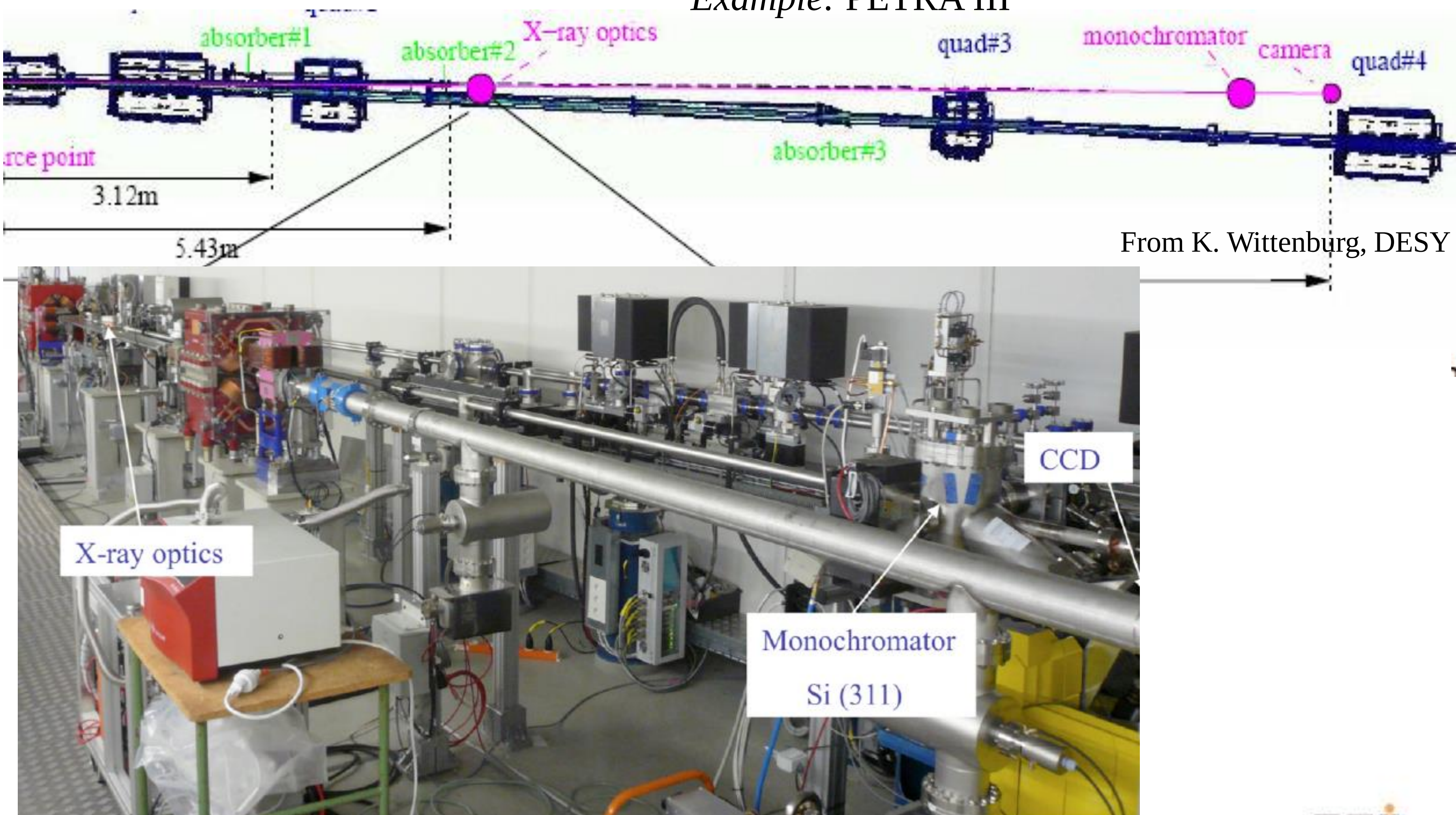

From K. Wittenburg, DESY

x-ray Pin-Hole Camera: Installation

The diffraction limit is $\Rightarrow \sigma \cong 0.6 \cdot \left(\lambda^2 / \rho\right)^{1/3}$ $\Rightarrow$ s***horter wavelength by x-rays***.

Example: PETRA III

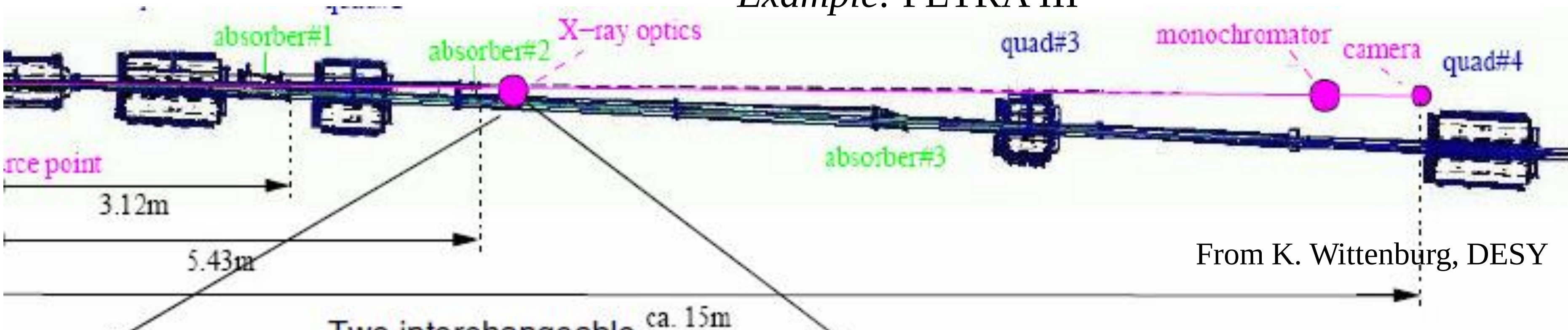

From K. Wittenburg, DESY

Two interchangeable X-ray optics:

Pinhole

0.5 mm thick tungsten blade with a circular hole of 20 μm. (20 μm resolution)

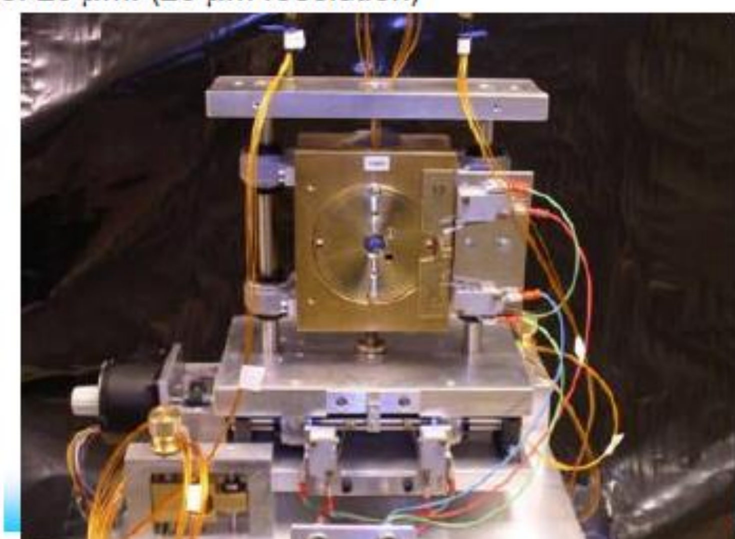

Compound reflective lens (RWTH Aachen)

N=31, ≈ 2 μm res. < 1 μm aligned

x-ray pin-hole Camera: x-ray Detector

x-ray optics → scintillator detector (shifting x-ray to optical light) → CCD camera

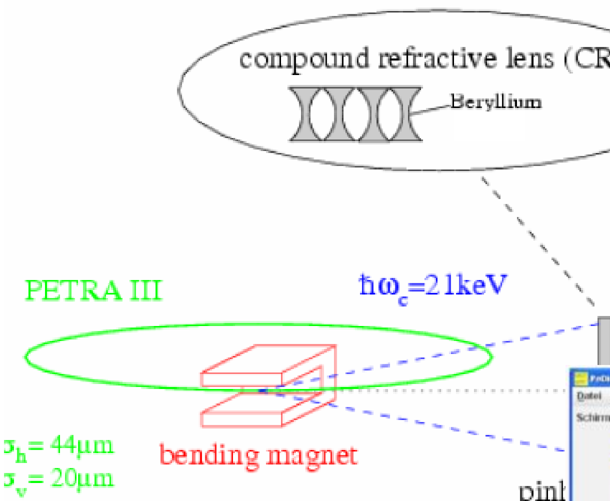

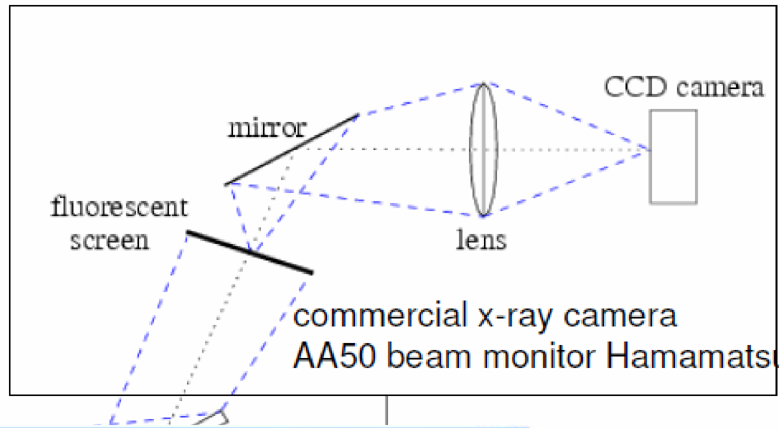

Example: PETRA III

- Pinhole with ∅ 20 µm or novel focusing device
- monochromator (silicon
- scintillator to convert x-ray to optical photons
- CCD sensor

From K. Wittenberg, DESY

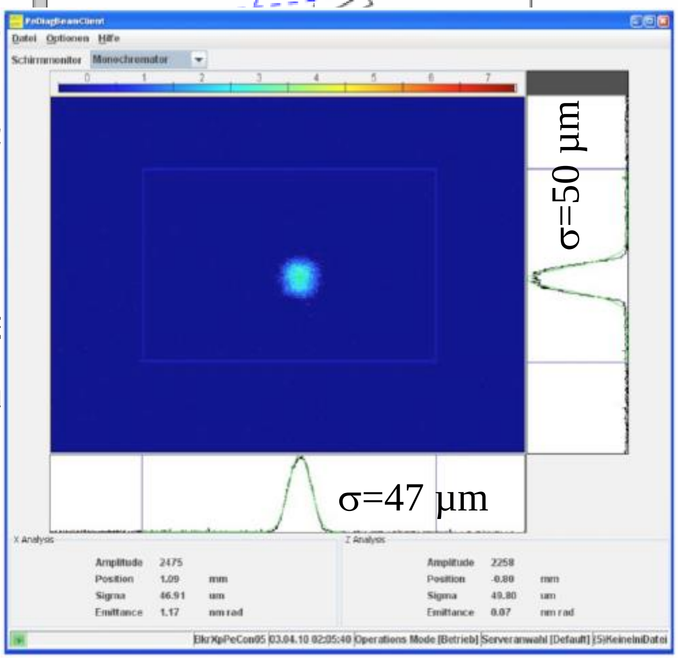

Commercial x-ray camera (Hamamatsu):

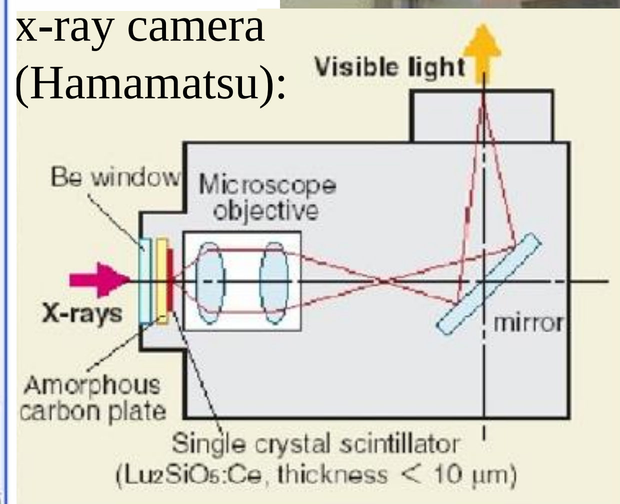

Summary for Beam Profile

Different techniques are suited for different beam parameters:

e⁻-beam: typically Ø 0.3 to 3 mm, **protons:** typically Ø 3 to 30 mm

Intercepting ↔ non-intercepting methods

Direct observation of electrodynamics processes:

- Optical synchrotron radiation monitor: non-destructive, for e^--beams, complex, limited res.
- X-ray synchrotron radiation monitor: non-destructive, for e^--beams, very complex
- OTR screen: nearly non-destructive, large relativistic γ needed, e^--beams mainly

Detection of secondary photons, electrons or ions:

- Scintillation screen: destructive, large signal, simple, all beams
- Ionization profile monitor: non-destructive, expensive, limited resolution, for protons
- Residual fluorescence monitor: non-destructive, limited signal strength, for protons

Wire based electronic methods:

- SEM-grid: partly destructive, large signal and dynamic range, limited resolution
- Wire scanner: partly destructive, large signal and dynamics, high resolution, slow scan.

Appendix: The Accelerator Facility at GSI

Ion Sources: all elements

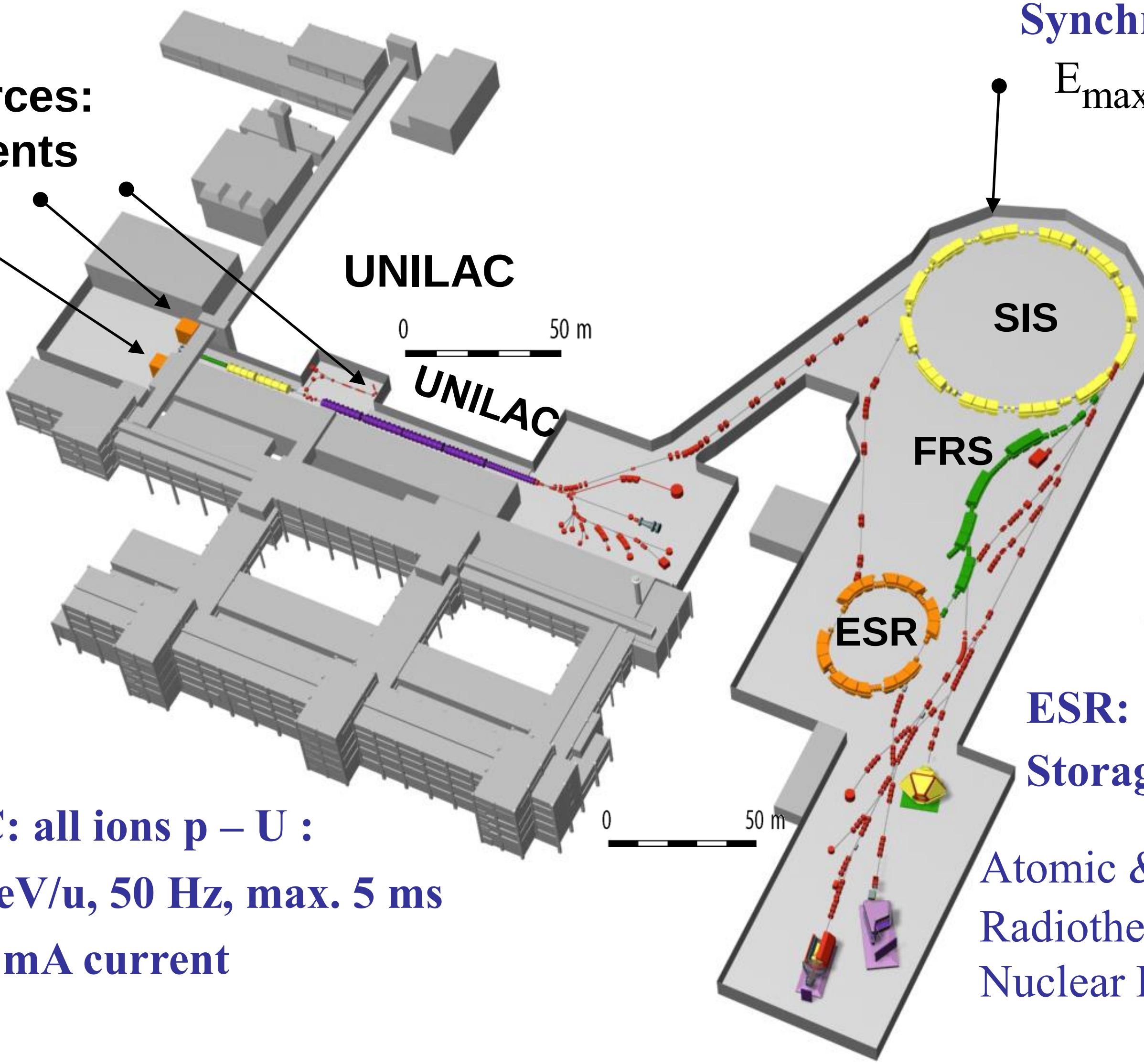

Synchrotron, Bρ=18 Tm

E_{max} p: 4.7 GeV

U: 1 GeV/u

Achieved e.g.:

Ar^{18+}: $1 \cdot 10^{11}$

U^{28+}: $3 \cdot 10^{10}$

U^{73+}: $1 \cdot 10^{10}$

UNILAC: all ions p – U :

3 – 12 MeV/u, 50 Hz, max. 5 ms

Up to 20 mA current

ESR:

Storage Ring, Bρ=10 Tm

Atomic & Plasma Physics

Radiotherapy

Nuclear Physics

SEM-Grid: Intersecting, high dynamic range, total 81 device

Beam Induced Fluorescence: Non-destructive, for high current operation total 6 device

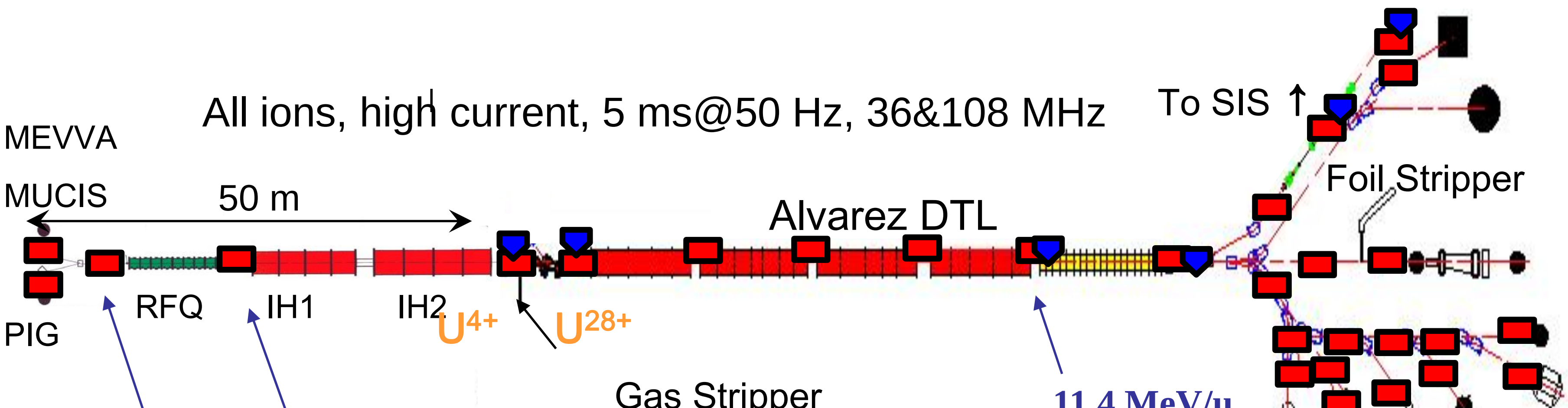

Gas Stripper

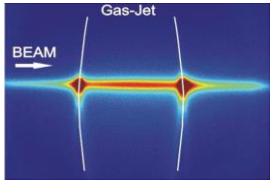

1.4 MeV/u ⇔β = 0.054

Constructed in the 70th, Upgrade 1999, further upgrades in preparation

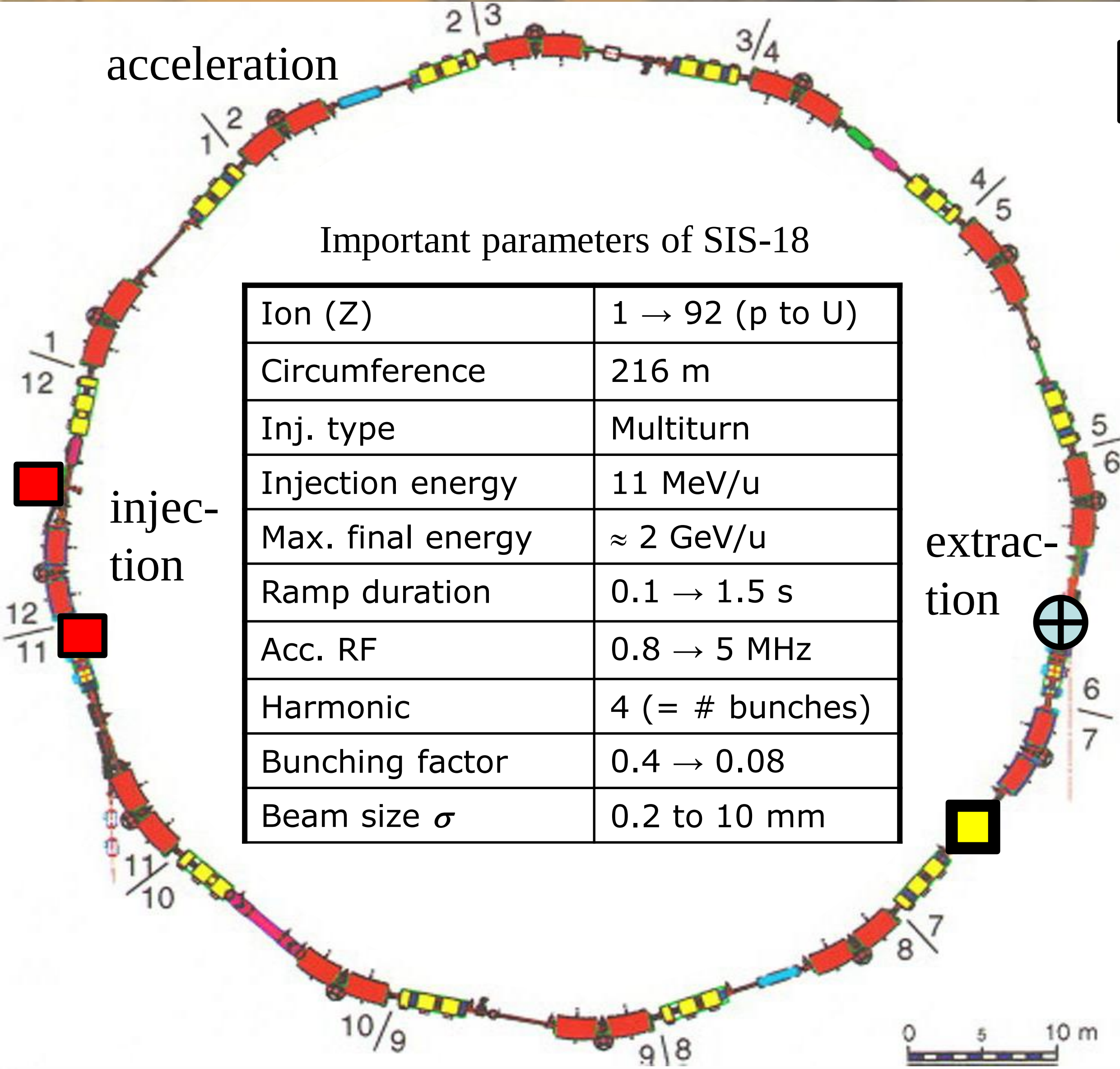

Important parameters of SIS-18

Ion (Z)	1 → 92 (p to U)
Circumference	216 m
Inj. type	Multiturn
Injection energy	11 MeV/u
Max. final energy	≈ 2 GeV/u
Ramp duration	0.1 → 1.5 s
Acc. RF	0.8 → 5 MHz
Harmonic	4 (= # bunches)
Bunching factor	0.4 → 0.08
Beam size σ	0.2 to 10 mm

SEM-Grid: injection
first turn
destructive

Screen: extraction
0.01... 500 MHz

IPM:
profile for stored beam
10 ms time resolution
non-destructive

3rd generation Spanish national synchrotron light facility in Barcelona

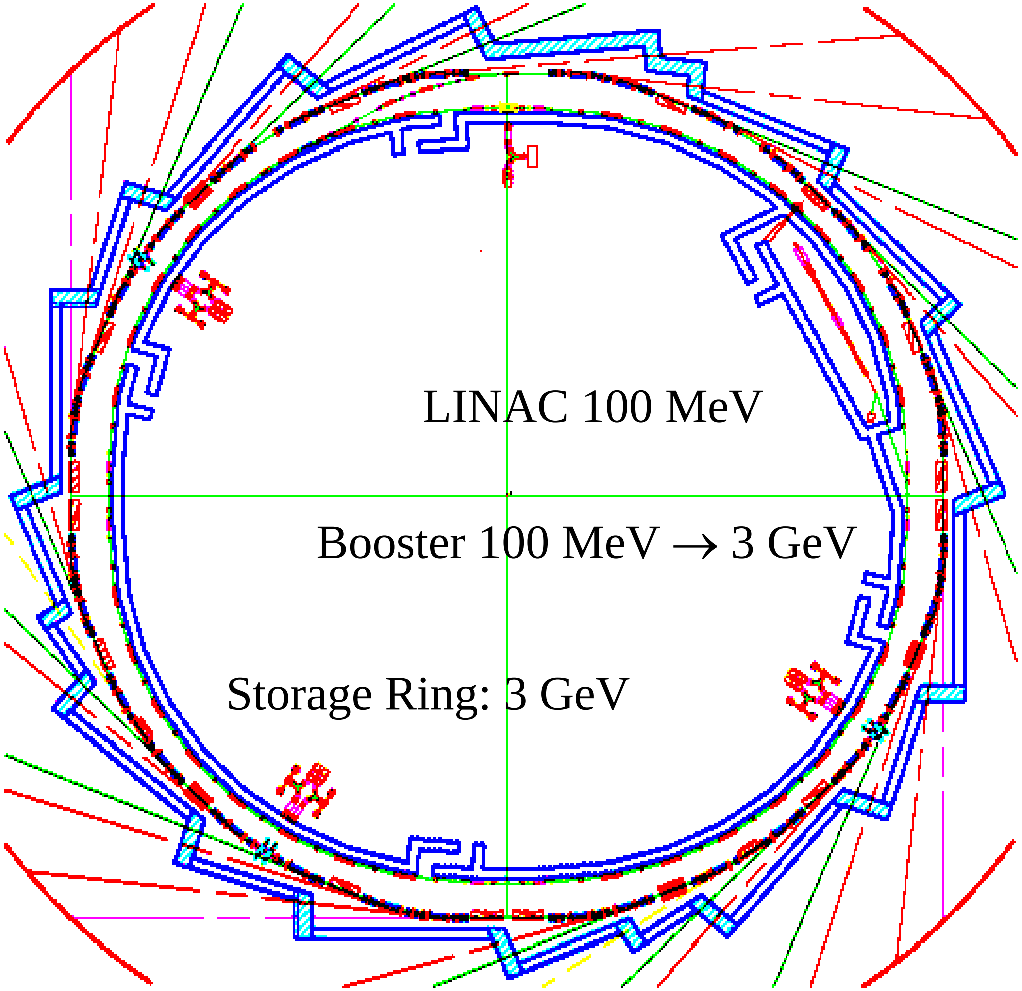

From U. Iriso, ALBA

Layout:

Beam lines: up to 30

Electron energy: 3 GeV

Top-up injection

Storage ring length: 268 m

Max. beam current: 0.4 A

Commissioning in 2011

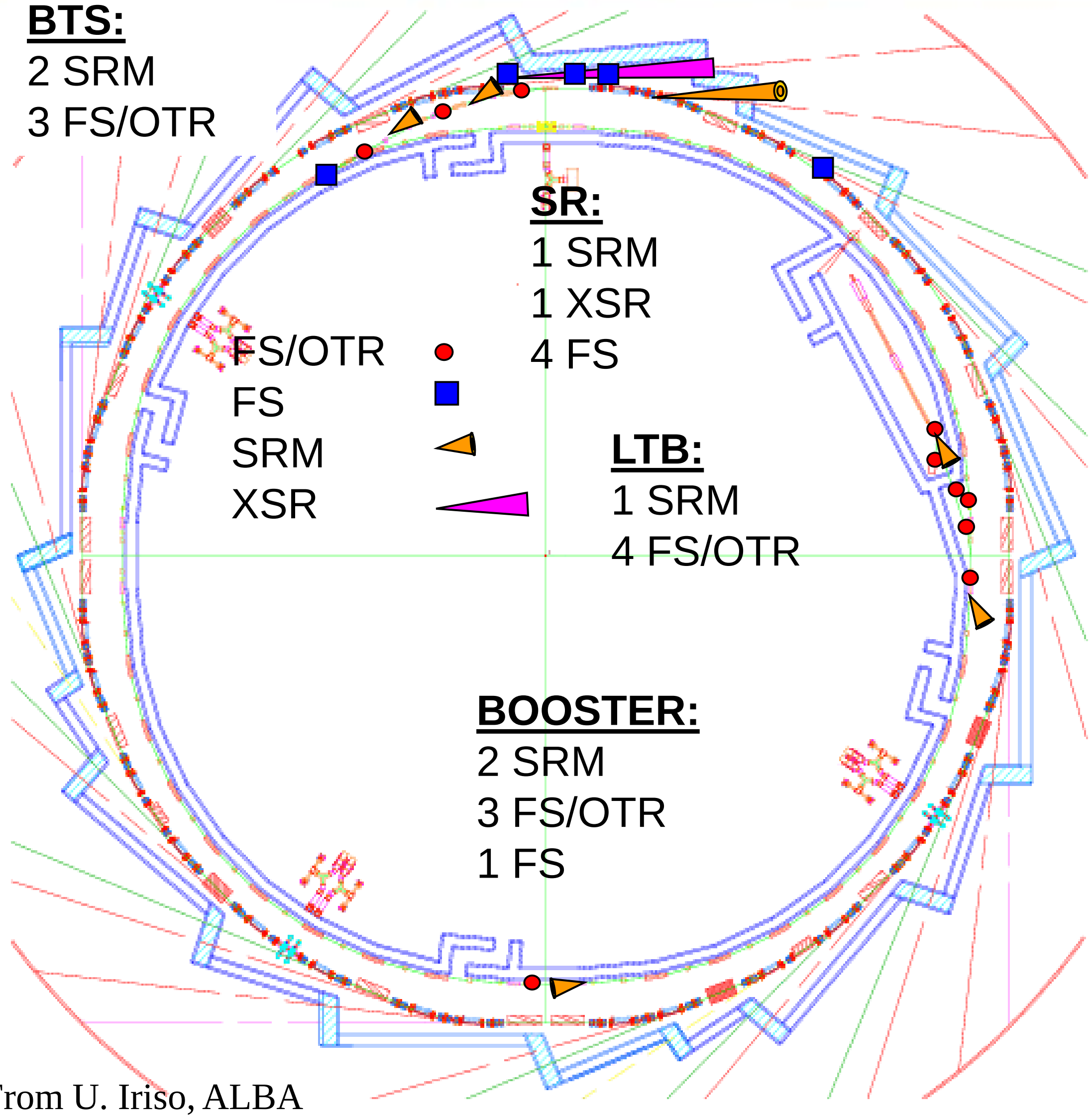

From U. Iriso, ALBA

Transverse profile:

Many location in transport line

Single location in ring

Quite different devices used

Abbreviation:

FS: Fluorescence Screen

OTR: Optical Trans. Radi. Screen

both destructive

SRM: Synchr. Radiation Monitor

XSR: X-ray pin hole camera

both **non-**destructive

Synchrotron Light Monitor overcoming Diffraction Limit

The diffraction limit is $\Rightarrow \sigma \cong 0.6 \cdot \left(\lambda^2 / \rho\right)^{1/3}$

Possible improvements:

- ***Shorter wavelength:*** Using x-rays and an aperture of Ø 1mm
  → 'x-ray pin hole camera'
- ***Interference technique:*** At optical wavelength using a double slit
  → interference fringes with resolution down to µm range.

Typical resolution for three methods:

- direct optical observation: $\sigma \approx$ **100 µ**
- interference optical obser: $\sigma \approx$ **1 µ**
- direct x-ray observation : $\sigma \approx$ **10 µ**

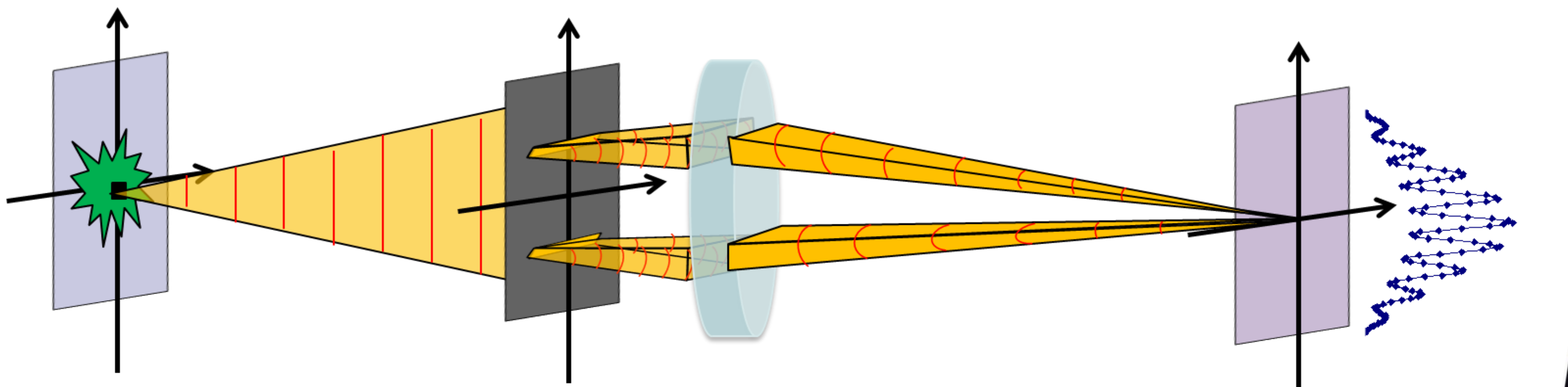

Synchrotron Light Monitor overcoming Diffraction Limit

The diffraction limit is $\Rightarrow \sigma \cong 0.6 \cdot \left(\lambda^2 / \rho\right)^{1/3}$

Possible improvements:

➢ ***Shorter wavelength:*** Using x-rays and an aperture of Ø 1mm ‘x-ray pin hole camera’

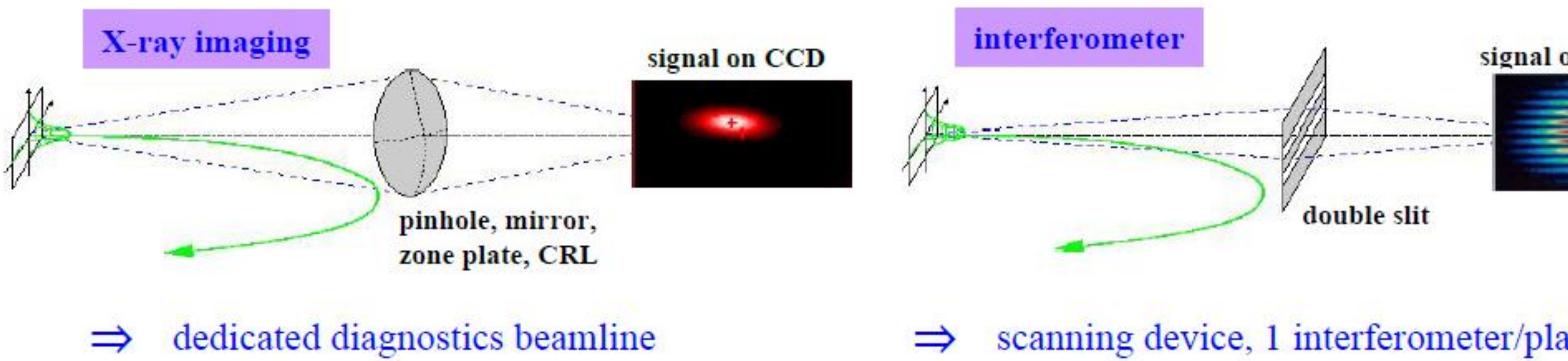

Ideal double slit interference pattern:

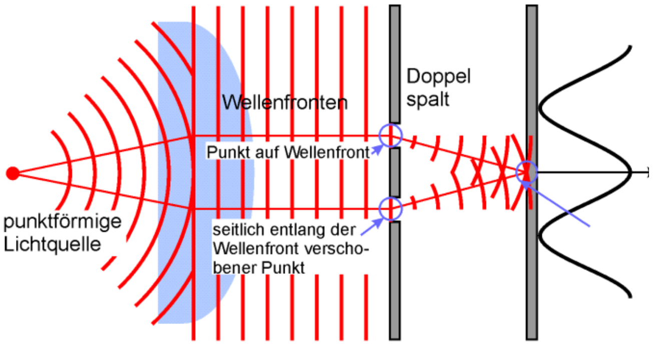

Blurring by finite source size

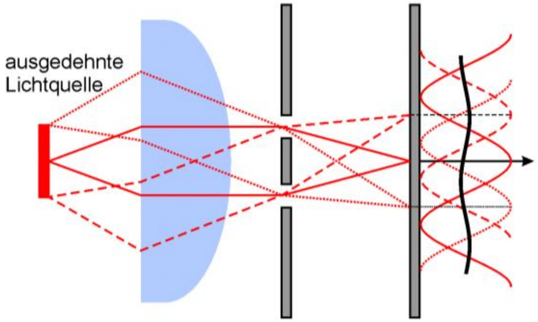

The **blurring of interference pattern** for finite size sources is described by Van-Cittert-Zernike-Theorem.

$\Rightarrow$ spatial coherence parameter γ delivers ***rms*** beam size i.e. 'de-convolution' of blurred image!

$\rightarrow$ highest resolution, but complex method

Typical resolution for three methods:

- direct optical observation: $\boldsymbol{\sigma \approx}$ **100 µm** (discussed before)
- interference optical obser: $\boldsymbol{\sigma \approx}$ **1 µm**
- direct x-ray observation : $\boldsymbol{\sigma \approx}$ **10 µm**

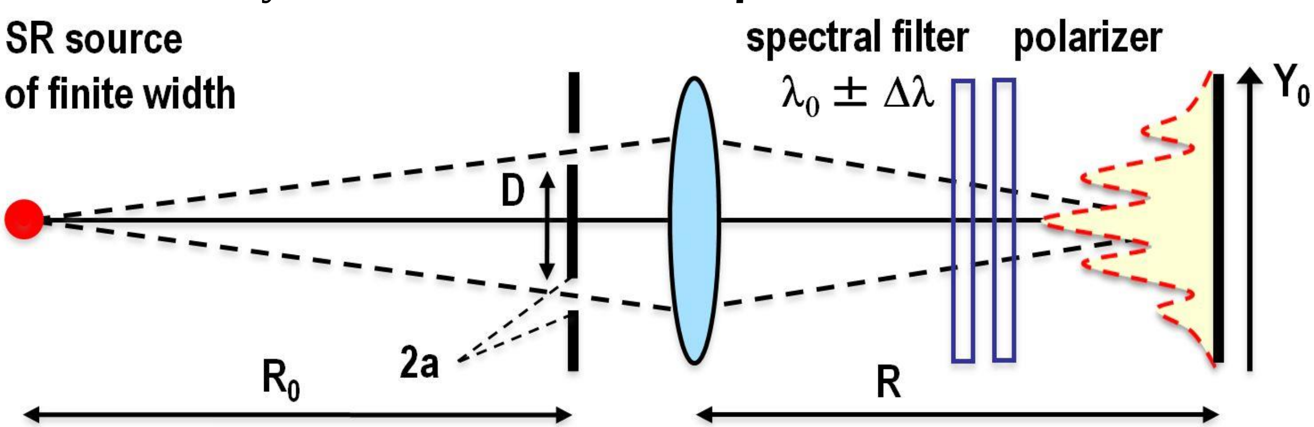

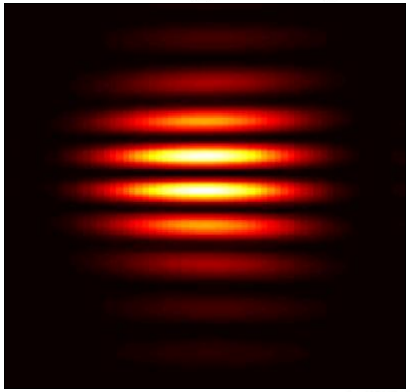

Courtesy of V. Schlott PSI